SUPPLEMENTARY INFORMATION

Organometallic Ru(II), Rh(III) and Re(I) complexes of sterane-based bidentate ligands: Synthesis, solution speciation, interaction with biomolecules and anticancer activity

Tamás Pivarcsik, Márton A. Kiss, Uroš Rapuš, Jakob Kljun, Gabriella Spengler, Éva Frank, Iztok Turel, Éva A. Enyedy*

Characterization of the organometallic complexes

Chemical shifts (δ) are reported in ppm. ^{1}H NMR spectra are referenced to residual peaks of NMR solvent $CDCl_3$ at 7.26 (referenced against the singlet line), and chemical shifts in ^{13}C NMR spectra relative to NMR solvent $CDCl_3$ at 77.16 (referenced against central line of triplet). The multiplicities are abbreviated as s = singlet, d = doublet, dd = doublet of the doublets dt = doublet of triplets and m = multiplet. Coupling constants (J) are given in Hz. MestReNova version 14.3 was used for NMR data processing.

[RhCp*(4-Me-bpy-St-OH)Cl]Cl (1)

^{1}H NMR ($CDCl_3$, δ/ppm, Figure S1.): 9.014 (d, J = 8.03 Hz, 0.46 H, H_{lig}(6'')), 8.904 (d, J = 8.08 Hz, 0.54 H, H_{lig}(6''), 8.771 (s, 0.46 H, H_{lig}(5')), 8.744 (s, 0.54 H, H_{lig}(5')), 8.685 (d, J = 5.11 Hz, 0.45 H, H_{lig}(3'')), 8.671 (d, J = 5.58 Hz, 0.55 H, H_{lig}(3'')), 8.298 (td, J = 7.88 Hz; J = 1.36 Hz, 0.46 H, H_{lig}(4'')), 8.269 (td, J = 8.02 Hz; J = 1.42 Hz, 0.54 H, H_{lig}(4'')), 7.651 (dd, J = 6.16 Hz; J = 0.79 Hz, 0.45 H, H_{lig}(5'')), 7.631 (dd, J = 6.48 Hz; J = 0.79 Hz, 0.55 H, H_{lig}(5'')), 3.686 (m, 1H, H_{lig}(17)), 3.701 (dd, J = 4.77 Hz, 0.50 H, H_{lig}(4)), 3.110 (dd, J = 18.85 Hz; 13.25 Hz, 0.50 H, H_{lig}(4)), 2.923 (dd, J = 18.89 Hz; 4.39 Hz, 0.50 H, H_{lig}(4)), 2.524 (dd, J = 17.05 Hz; 12.56 Hz, 0.50 H, H_{lig}(4)), 2.841 (dd, J = 17.31 Hz; 7.13 Hz, 1H, H_{lig}(1)), 2.380 (d, J = 16.91 Hz; 0.50 H, H_{lig}(1)), 2.272 (d, J = 17.57 Hz; 0.50 H, H_{lig}(1)), 2.551 (d, J = 5.22 Hz; 3H, H_{lig}(1''')), 2.095 (m, 1H, H_{lig}(5)), 1.913 (m, 1H), 1.844 – 1.625 (m-s, 6H), 1.584 (s, 7H, $HC_5Me_5(CH_3)$), 1.557 (s, 8H, $HC_5Me_5(CH_3)$), 1.519 – 1.254 (m-s, 10H), 1.160 (t, J = 11.94 Hz, 1H), 1.046 – 0.821 (m-s, 6H), 0.935; 0.803; 0.782; 0.741 (s-s, 6H, H_{lig}(18, 19)).

^{13}C NMR ($CDCl_3$, δ/ppm, Figure S2.): 158.77 (C(3)), 158.50 (C(3)), 156.59 (C(2'')), 156.29 (C(2'')), 152.49 (C(6')), 152.40 (C(6')), 151.99 (C(6'')), 151.97 (C(6'')), 151.91 (C(4')), 151.46 (C(4')), 141.23 (C(4'')), 141.14 (C(4'')), 136.52 (C(2)), 136.47 (C(2)), 127.19 (C(5')), 125.03 (C(5'')), 124.87 (C(5'')), 124.26 (C(3'')), 124.19 (C(3'')), 97.00 (C(C_5)), 96.94 (C(C_5)), 81.70 (C(17)), 81.68 (C(17)), 53.75 (C(9)), 53.67 (C(9)), 50.88 (C(14)), 50.77 (C(14)), 42.86 (C(13)), 42.85 (C(13)), 42.31 (C(13)), 41.23 (C(5)), 41.01 (C(5)), 40.72 (C(5)), 39.37 (C(1)), 38.08 (C(1)), 36.59 (C(12)), 36.53 (C(12)), 35.49 (C(10)), 35.45 (C(10)), 35.37 (C(4)), 34.42 (C(8)), 31.04 (C(7)), 30.81 (C(7)), 30.44 (C(16)), 30.42 (C(16)), 27.98 (C(6)), 27.90 (C(6)), 23.38 (C(15)), 23.36 (C(15)), 20.99 (C(11)), 19.80 (C(1''')), 19.76 (C(1''')), 12.94 (C(18)), 12.68 (C(18)), 11.14 (C(19)), 11.12 (C(19)), 9.72 (C(Me_5)), 9.37 (C(Me_5)).

ESI-HRMS (positive): calc. for [RhCp*(4-Me-bpy-St-OH)Cl]$^{+}$ ($C_{38}H_{51}ClN_2ORh$): 689.2745 (m/z) found: 689.2727 (m/z).

Synthesis of [RhCp*(4-Ph-bpy-St-OH)Cl]Cl (2)

^{1}H NMR ($CDCl_3$, δ/ppm, Figure S3.): 8.792 (dd, 1H, H_{lig}(3'')), 8.404 (dd, 1H, H_{lig}(6'')), 8.685 (d, J = 5.11 Hz, 1H, H_{lig}(4'')), 8.055 (s, 0.56 H, H_{lig}(5')), 8.027 (s, 0.44 H, H_{lig}(5')), 7.743 (ddd, 1H, H_{lig}(5'')), 7.555 (td, J = 7.80 Hz; J = 1.74 Hz, 2H, H_{lig}(3''' & 5''')), 7.512 (m, 1H, H_{lig}(4''')), 7.400 (dd, J = 14.26 Hz; J = 7.10 Hz, 2H, H_{lig}(2''' & 6''')), 3.856 (dd, J = 18.09; J = 5.44, 4.87 Hz, 0.46 H, H_{lig}(4)), 3.640 (q, J = 19.33 Hz; J = 8.58 Hz, 1H, H_{lig}(17)), 3.201 (d, J = 12.62 Hz, 0.20 H, H_{lig}(4)), 3.168 (d, J = 13.02 Hz, 0.40 H, H_{lig}(4)), 3.111 (d, J = 4.88 Hz, 0.38 H, H_{lig}(4)), 3.079 (d, J = 4.97 Hz, 0.19 H, H_{lig}(4)), 2.863 (d, J = 17.47 Hz, 0.50 H, H_{lig}(1)), 2.792 (d, J = 17.11 Hz, 0.50 H, H_{lig}(1)), 2.623 (dd, J = 17.75; J = 11.86 Hz, 0.50 H, H_{lig}(4)), 2.537 (d, J = 16.94 Hz, 0.50 H, H_{lig}(1)), 2.333 (d, J = 16.58 Hz, 0.50 H, H_{lig}(1)), 2.077 (m, 1H, H_{lig}(5)), 1.915 – 1.695 (m-s, 6H), 1.673 (s, 7H, $HC_5M_{e5}(CH_3)$), 1.655 (s, 8H, $HC_5Me_5(CH_3)$), 1.481 – 1.254 (m-s,

13H), 1.091 – 0.938 (m-s, 4H), 0.856 – 0.779 (m-s, 2H), 0.883; 0.736; 0.704; 0.654 (s-s, 6H, H_{lig}(18, 19)).

^{13}C NMR ($CDCl_3$, δ/ppm, Figure S4.): 160.62 (C(3)), 160.54 (C(3)), 155.97 (C(2'')), 155.72 (C(2'')), 154.49 (C(6')), 154.31 (C(6')), 152.45 (C(4')), 151.97 (C(4')), 151.97 (C(6'')), 151.92 (C(6'')), 141.00 (C(1''')), 141.95 (C(1''')), 136.64 (C(4'')), 136.45 (C(4'')), 135.38 (C(2)), 135.19 (C(2)), 129.49 (C(4''')),129.35 (C(4''')), 129.04 (C(3''' & 5''')), 128.48 (C(2''' & 6''')), 128.31 (C(2''' & 6''')), 127.69 (C(5'')), 127.65 (C(5'')), 123.93 (C(3'')), 123.71 (C(3'')), 122.78 (C(5')),1 22.38 (C(5')), 97.52 (C(C_5), 97.49 (C(C_5)), 97.47 (C(C_5), 97.44 (C(C_5)), 81.71 (C(17)), 53.37 (C(9)), 53.35 (C(9)), 50.78 (C(14)), 50.72 (C(14)), 42.77 (C(13)), 42.36 (C(13)), 42.11 (C(5)), 42.04 (C(5)), 40.07 (C(1)), 38.85 (C(1)), 36.46 (C(12)), 36.43 (C(12)), 35.78 (C(10)), 35.47 (C(4)), 35.36 (C(4)), 34.63 (C(8)), 30.96 (C(7)), 30.81 (C(7)), 30.46 (C(16)), 28.00 (C(6)), 23.36 (C(15)), 23.34 (C(15)), 20.83 (C(11)), 12.43 (C(18)), 12.15 (C(18)), 11.05 (C(19)), 11.03 (C(19)), 10.00 (C(Me_5)), 9.63 (C(Me_5)).

ESI-HRMS (positive): calc. for [RhCp*(4-Ph-bpy-St-OH)Cl]$^+$ ($C_{43}H_{53}ClN_2ORh$): 751.2901 (m/z) found: 751.2883 (m/z).

Synthesis of [RuCym(4-Me-bpy-St-OH)Cl]Cl (3)

^{1}H NMR ($CDCl_3$, δ/ppm, Figure S5.): 9.682 (m, 0.38 H, H_{lig}(3'')), 9.544 (m, 0.62 H, H_{lig}(3'')), 8.232 (dd, J = 8.11 Hz, 0.38 H, H_{lig}(6'')), 8.214 (dd, J = 8.35 Hz, 0.62 H, H_{lig}(6'')), 8.043 (m, 1H, H_{lig}(4'')), 8.019 (s, 0.38 H, H_{lig}(5')), 7.992 (s, 0.62 H, H_{lig}(5')), 7.777 (m, 0.38 H, H_{lig}(5'')), 7.730 (m, 0.62 H, H_{lig}(5'')), 6.274 (m, 0.38 H, H_{Cym}(C3)), 6.100 (m, 0.62 H, H_{Cym}(C3)), 6.035 (m, 1H, H_{Cym}(C3)), 5.941 (d, 0.62 H, H_{Cym}(C2)), 5.851 (d, 0.38 H, H_{Cym}(C2)), 5.686 (d, 0.62 H, H_{Cym}(C2)), 5.638 (d, 0.38 H, H_{Cym}(C2)), 3.712 (dd, J = 4.48 Hz, 0.38 H, H_{lig}(4)), 3.692 (m, 1H, H_{lig}(17)), 3.346 (dd, J = 18.38; 5.23 Hz, 0.62 H, H_{lig}(4)), 3.190 (dd, J = 18.27; 12.73 Hz, 0.62 H, H_{lig}(4)), 2.821 (dd, Under the peak H_{lig}(1), 0.38 H, H_{lig}(4)), 2.836 (d, J = 17.63 Hz, 0.38 H, H_{lig}(1)), 2.792 (d, J = 16.96 Hz, 0.62 H, H_{lig}(1)), 2.601 – 2.501 (m, 1H, H_{Cym}(C5)), 2.466 (s, 1H, H_{Cym}(C8)), 2.461 (s, 2H, H_{Cym}(C8)), 2.417 (d, J = 16.84 Hz, 0.62 H, H_{lig}(1)), 2.303 (d, J = 11.81 Hz, 0.62 H, H_{lig}(1)), 2.280 (s, 1H, H_{lig}(1''')), 2.232 (s, 2H, H_{lig}(1''')), 2.104 (m, 1H, H_{lig}(5)), 1.956 – 1.878 (m, 2H), 1.860 – 1.781 (m, 2H), 1.759 – 1.682 (m, 3H), 1.539 – 1.141 (m, Sterane protons), 1.061 – 1.003 (d-s, 6H, H_{Cym}(C6 & C7)), 0.884 (s, 1H, H_{lig}(18)), 0.819 (s, 1H, H_{lig}(19)), 0.780 (s, 2H, H_{lig}(18)), 0.681 (s, 2H, H_{lig}(19)).

^{13}C NMR ($CDCl_3$, δ/ppm, Figure S6.): 160.40 (C(3)), 160.06 (C(3)), 157.13 (C(2'')), 156.65 (C(2'')), 155.55 (C(6')), 154.94 (C(6')), 152.57 (C(6'')), 152.40 (C(6'')), 151.09 (C(4')), 150.82 (C(4')), 139.71 (C(4'')), 139.63 (C(4'')), 136.05 (C(2)), 135.76 (C(2)), 128.22 (C(5')), 127.83 (C(5')), 123.08 (C(5'')), 122.96 (C(3'')), 122.86 (C(3'')), 105.75 (C(C4)),104.12 (C(C1)),88.65 (C(C3 & C2)),85.85 (C(C3 & C2)),84.08 (C(C3 & C2)),83.64 (C(C3 & C2)), 81.78 (C(17)), 81.72 (C(17)), 53.91 (C(9)), 53.62 (C(9)), 50.87 (C(14)), 50.81 (C(14)), 42.90 (C(13)), 42.88 (C(13)), 42.18 (C(13)), 41.37 (C(1)), 41.32 (C(1)), 41.13 (C(1)), 40.06 (C(5)), 40.02 (C(5)), 36.64 (C(12)), 36.58 (C(12)), 35.47 (C(10)), 34.76 (C(4)), 34.20 (C(8)), 31.13 (C(7)), 31.05 (C(7)), 30.95 (C(C5)), 30.82 (C(C5)), 30.51 (C(16)), 30.46 (C(16)), 28.41 (C(6)), 28.26 (C(6)), 23.38 (C(15)), 22.50 (C(C6 & C7)), 22.31 (C(C6 & C7)), 22.11 (C(C6 & C7)), 21.79 (C(C6 & C7)), 21.05 (C(11)), 21.01 (C(11)), 19.90 (C(1''')), 19.80 (C(1''')), 19.12 (C(C8)), 18.90 (C(C8)), 12.79 (C(18)), 12.31 (C(18)), 11.19 (C(19)), 11.15 (C(19)).

ESI-HRMS (positive): calc. for [RuCym(4-Me-bpy-St-OH)Cl]$^+$ ($C_{38}H_{50}ClN_2ORu$): 687.2655 (m/z) found: 687.2641 (m/z).

Synthesis of [RuCym(4-Ph-bpy-St-OH)Cl]Cl (4)

^{1}H NMR ($CDCl_3$, δ/ppm, Figure S7.): 9.860 (m, 0.33 H, H_{lig}(3'')), 9.716 (m, 0.67 H, H_{lig}(3'')), 8.020 (dd, 0.33 H, H_{lig}(6'')), 8.014 (dd, 0.67 H, H_{lig}(6'')), 8.014 (t, Under the peak H_{lig}(6''), 0.67 H, H_{lig}(4'')), 7.975 (t, J = 7.91; 9.38 Hz, 0.33 H, H_{lig}(4'')), 7.858 (m, 0.33 H, H_{lig}(5'')), 7.806 (m, 0.67 H, H_{lig}(5'')), 7.788 (s, 0.67 H, H_{lig}(5')), 7.747 (s, 0.33 H, H_{lig}(5')), 7.556 – 7.505 (m, 3H, H_{lig}(3''' – 5''')), 7.343 (d, J = 6.53 Hz, 2H, H_{lig}(2''' & 6''')), 7.290 (d, J = 6.53 Hz, 1H, H_{lig}(2''' & 6''')), 6.449 (m, 0.38 H, H_{Cym}(C3)), 6.228 (m, 1H, H_{Cym}(C3)), 6.214 (m, 0.67 H, H_{Cym}(C3)), 6.134 (d, J = 4.97 Hz, 0.67 H, H_{Cym}(C2)), 5.962 (d, J = 5.63 Hz, 0.33 H, H_{Cym}(C2)), 5.823 (d, J = 5.18 Hz, 0.67 H, H_{Cym}(C2)), 5.771 (d, J = 3.91 Hz, 0.33 H, H_{Cym}(C2)), 3.854 (dd, J = 17.42, 4.74 Hz, 0.33 H, H_{lig}(4)), 3.636 (m, J = 14.03 Hz, 8.07 Hz, 7.74 Hz, 1H, H_{lig}(17)), 3.538 (dd, J = 18.50, 5.83, 6.00 Hz, 0.67 H, H_{lig}(4)), 3.292 (dd, J = 18.66, 11.67 Hz, 12.04, 0.67 H, H_{lig}(4)), 2.904 (dd, J = 17.34, 12.15 Hz, 12.47, 0.33 H, H_{lig}(4)), 2.838 (d, J = 17.58 Hz, 0.33 H, H_{lig}(1)), 2.702 (d, J = 16.73 Hz, 0.67 H, H_{lig}(1)), 2.626 (m, 1H, H_{Cym}(C5)), 2.562 (d, J = 16.74 Hz, 0.67 H, H_{lig}(1)),

2.315 (s, 1H, H_{Cym}(C8)), 2.295 (d, Under the peak H_{Cym}(C8), 0.33 H, H_{lig}(1)), 2.270 (s, 2H, H_{Cym}(C8)), 2.068 (m, 1H, H_{lig}(5)), 2.060 – 2.020 & 1.829 – 1.729 (m, 4H), 1.464 – 1.229 (m, 10H), 1.089 – 1.050 (d-s, 6H, H_{Cym}(C6 & C7)), 0.959 (s, 1H, H_{lig}(18)), 0.750 (s, 1H, H_{lig}(19)), 0.695 (s, 2H, H_{lig}(18)), 0.564 (s, 2H, H_{lig}(19)).

^{13}C NMR ($CDCl_3$, δ/ppm, Figure S8.): 162.61 (C(3)), 161.58 (C(3)), 157.97 (C(2'')), 157.29 (C(2'')), 155.20 (C(6')), 154.49 (C(6')), 153.66 (C(4')), 153.68 (C(4')), 152.80 (C(6'')), 152.49 (C(6'')), 139.39 (C(1''')), 139.32 (C(1''')), 136.84 (C(4'')), 136.74 (C(4'')), 134.97 (C(2)), 134.52 (C(2)), 129.43 (C(4''')), 129.31 (C(4''')), 129.06 (C(3''' & 5''')), 129.02 (C(3''' & 5''')), 128.76 (C(5'')), 128.23 (C(5'')), 128.39 (C(2''' & 6''')), 128.08 (C(2''' & 6''')), 122.26 (C(3'')), 122.16 (C(3'')), 121.61 (C(5')),121.46 (C(5')), 106.33 (C(C4)), 104.09 (C(C1)), 88.84 (C(C3 & C2)), 86.60 (C(C3 & C2)), 84.07 (C(C3 & C2)), 83.80 (C(C3 & C2)), 81.78 (C(17)), 81.71 (C(17)), 53.52 (C(9)), 53.23 (C(9)), 50.78 (C(14)), 50.73 (C(14)), 42.82 (C(13)), 42.79 (C(13)), 42.64 (C(13)), 42.44 (C(1)), 42.34 (C(1)), 41.49 (C(1)), 40.70 (C(5)), 40.66 (C(5), 36.52 (C(12)), 36.46 (C(12)), 35.47 (C(10)), 35.45 (C(10)), 35.01 (C(4)), 34.37(C(8)), 31.24 (C(7)), 31.14 (C(7)), 30.89 (C(C5)), 30.81 (C(C5)), 30.51 (C(16)), 30.46 (C(16)), 28.45 (C(6)), 28.33 (C(6)), 23.36 (C(15)), 22.55 (C(C6 & C7)), 22.29 (C(C6 & C7)), 22.18 (C(C6 & C7)), 21.85 (C(C6 & C7)), 20.87 (C(11)), 20.80 (C(11)), 19.16 (C(C8)), 18.95 (C(C8)), 12.36 (C(18)), 11.86 (C(18)), 11.09 (C(19)), 11.05 (C(19)).

ESI-HRMS (positive): calc. for [RuCym(4-Ph-bpy-St-OH)Cl]$^+$ ($C_{43}H_{52}ClN_2ORu$): 749.2812 (m/z) found: 749.2798 (m/z).

Synthesis of [Re(CO)$_3$(4-Me-bpy-St-OH)Cl]Cl (5)

^{1}H NMR ($CDCl_3$, δ/ppm, Figure S9.): 9.092 (td, J = 4.92 Hz; J = 0.83 Hz, 1H, H(3'')), 8.114 (t, J = 7.93 Hz; 1H, H(6'')), 7.998 (td, J = 7.89 Hz; J = 1.55, 1.44 Hz, 1H, H(4'')), 7.802 (d, J = 7.30 Hz; 1H, H(5')), 7.468 (m, J = 1.16 Hz, 1H, H(5'')), 3.676 (m, 1H, H(17)), 3.523 (dd, J = 17.85; 5.36 Hz, 0.50 H, H(4)), 3.260 (dd, J = 17.83; 5.16 Hz, 0.50 H, H(4)), 3.128 (dd, J = 17.85; 12.26 Hz, 0.50 H, H(4)), 2.930 (dd, J = 17.84; 12.29 Hz, 0.50 H, H(4)), 2.773 (dd, J = 17.13; 5.94 Hz, 1H, H(1)), 2.409 (s, 3H, H(1''')), 2.314 (dd, J = 16.00, 1H, H(1)), 2.098 (m, 1H, H(5)), 1.902 (dq, 1H), 1.811 (m, 2H), 1.727 – 1.626 (m, 3H), 1.527 – 1.428 (m-s, 4H), 1.352 – 1.282 (m-s, 2H), 1.190 – 1.129 (m-s, 1H), 1.051 – 0.858 (m-s, 4H), 0.843 (d, J = 4.34, 3H, H(18)), 0.796 (d, J = 1.64, 3H, H(19)).

^{13}C NMR ($CDCl_3$, δ/ppm, Figure S10.): 197.47 , 197.40, 197.09 (C(C1 – C3)), 159.46 (C(3)), 159.21 (C(3)), 157.40 (C(2'')), 157.21 (C(2'')), 152.95 (C(6')), 152.83 (C(6')), 152.71 (C(6'')), 152.67 (C(6'')), 150.06 (C(4')), 150.05 (C(4')), 138.69 (C(4'')), 135.25 (C(2)), 135.17 (C(2)), 126.32 (C(5')), 126.07 (C(5')), 122.72 (C(5'')), 122.59 (C(5'')), 122.27 (C(3'')),122.14 (C(3'')), 81.93 (C(17)), 81.89 (C(17)), 53.97 (C(9)), 53.85 (C(9)), 50.93 (C(14)), 50.86 (C(14)), 42.98, 42.88, 42.49, 42.43, 42.12, 41.44 (C(13 & 5 & 1)), 36.70 (C(12)), 36.67 (C(10)), 35.52 (C(4)), 35.45 (C(4)), 34.23 (C(8)), 34.11 (C(8)), 30.97 (C(7)), 30.94 (C(7)), 30.89 (C(7)), 30.61 (C(16)), 30.59 (C(16)), 27.80 (C(6)), 27.72 (C(6)), 23.38 (C(15)), 21.07 (C(11)), 20.07 (C(1''')), 20.01 (C(1''')), 12.34 (C(18)), 12.22 (C(18)), 11.14 (C(19)), 11.12 (C(19)).

ESI-HRMS (positive): calc. for [Re(CO)$_3$(4-Me-bpy-St-OH)CH_3CN] ($C_{33}H_{42}N_3O_4Re$): 728.2498 (m/z) found: 728.2488 (m/z).

Synthesis of [Re(CO)$_3$(4-Ph-bpy-St-OH)Cl]Cl (6)

^{1}H NMR ($CDCl_3$, δ/ppm, Figure S11.): 9.125 (dq, J = 5.53 Hz, 0.90 H, H(3'')), 9.102 (d, J = 5.08 Hz, 0.05 H, H(3'')), 9.078 (d, J = 4.89 Hz, 0.05 H, H(3'')), 8.179 (t, J = 7.83 Hz, 0.10 H, H(6'')), 8.102 (t, J = 8.46 Hz, 0.90 H, H(6'')), 8.102 (Under the peak H(6''), 0.10 H, H(4'')), 7.987 (td, J = 7.74 Hz; J = 1.40 Hz, 0.90 H, H(4'')), 7.917 (s, 0.06 H, H(5')), 7.888 (s, 0.04 H, H(5')), 7.840 (d, J = 9.94 Hz, 0.90 H, H(5')), 7.626 – 7.563 (0.20 H, H(5'', 3''', 4''', 5''')), 7.557 – 7.470 (4H, H(5'', 3''', 4''', 5''')), 7.376 – 7.353 (0.20 H, H(2''' & 6''')), 7.339 (dt, J = 6.61 Hz, 0.95 H, H(2''' & 6''')) and 7.312 (dt, J = 6.53 Hz, 0.85 H, H(2''' & 6''')), 3.665 (dd, J = 18.82; 5.75 Hz, 0.50 H, H(4)), 3.624 (m, 1H, H(17)), 3.433 (dd, J = 17.32; 5.43 Hz, 0.50 H, H(4)), 3.159 (dd, J = 18.00; 12.17 Hz, 0.50 H, H(4)), 2.969 (dd, J = 18.02; 11.78 Hz, 0.50 H, H(4)), 2.751 (dd, J = 17.08; 8.25 Hz, 1H, H(1)), 2.374 (d, J = 22.25; 17.22 Hz, 1H, H(1)), 2.072 (m, 1H, H(5)), 1.852 – 1.601 (m-s, 6H), 1.491 – 1.254 (m-s, 10H), 1.067 – 0.779 (m-s, 6H), 0.755 (d, J = 6.03 Hz, 3H, H(18)), 0.722 (d, J = 3.00 Hz, 3H, H(19))

^{13}C NMR ($CDCl_3$, δ/ppm, Figure S12.): 197.40, 197.33, 196.98 (C(C1 – C3)), 160.82 (C(3)), 160.61 (C(3)), 157.30 (C(2'')), 157.13 (C(2'')), 153.26 (C(6')), 153.21 (C(6')), 153.19 (C(4')), 153.15 (C(4')), 152.77 (C(6'')), 152.74 (C(6'')), 138.77 (C(1''')), 138.74 (C(1''')), 137.54 (C(4'')), 137.51 (C(4'')), 134.14 (C(2)), 133.95 (C(2)), 129.11, 128.99, 128.97, 128.16, 128.08 (C(2''' – 6''')), 126.51 (C(5'')), 126.30

(C(5'')), 122.88 (C(3'')), 122.76 (C(3'')), 121.98 (C(5')),121.80 (C(5')), 81.92 (C(17)), 81.87 (C(17)), 53.60 (C(9)), 53.46 (C(9)), 50.86 (C(14)), 50.78 (C(14)), 43.58 (C(5)), 43.13 (C(5)), 42.80 (C(13)), 42.77 (C(1)), 42.66 (C(1)), 42.55 (C(1)), 42.43 (C(1)), 36.58 (C(12)), 36.54 (C(12)), 35.52 (C(4)), 35.45 (C(4)), 35.42 (C(8)), 35.33 (C(8)), 30.95 (C(7)), 30.87 (C(7)), 30.60 (C(16)), 30.57 (C(16)), 27.85 (C(6)), 27.82 (C(6)), 23.36 (C(15)), 20.87 (C(11)), 20.86 (C(11)), 11.86 (C(18)), 11.80 (C(18)), 11.06 (C(19)), 11.03 (C(19)).
ESI-HRMS (positive): calc. for $[Re(CO)_3(4\text{-Ph-bpy-St-OH})CH_3CN]$ ($C_{38}H_{44}N_3O_4Re$): 790.2655 (m/z) found: 790.2636 (m/z).

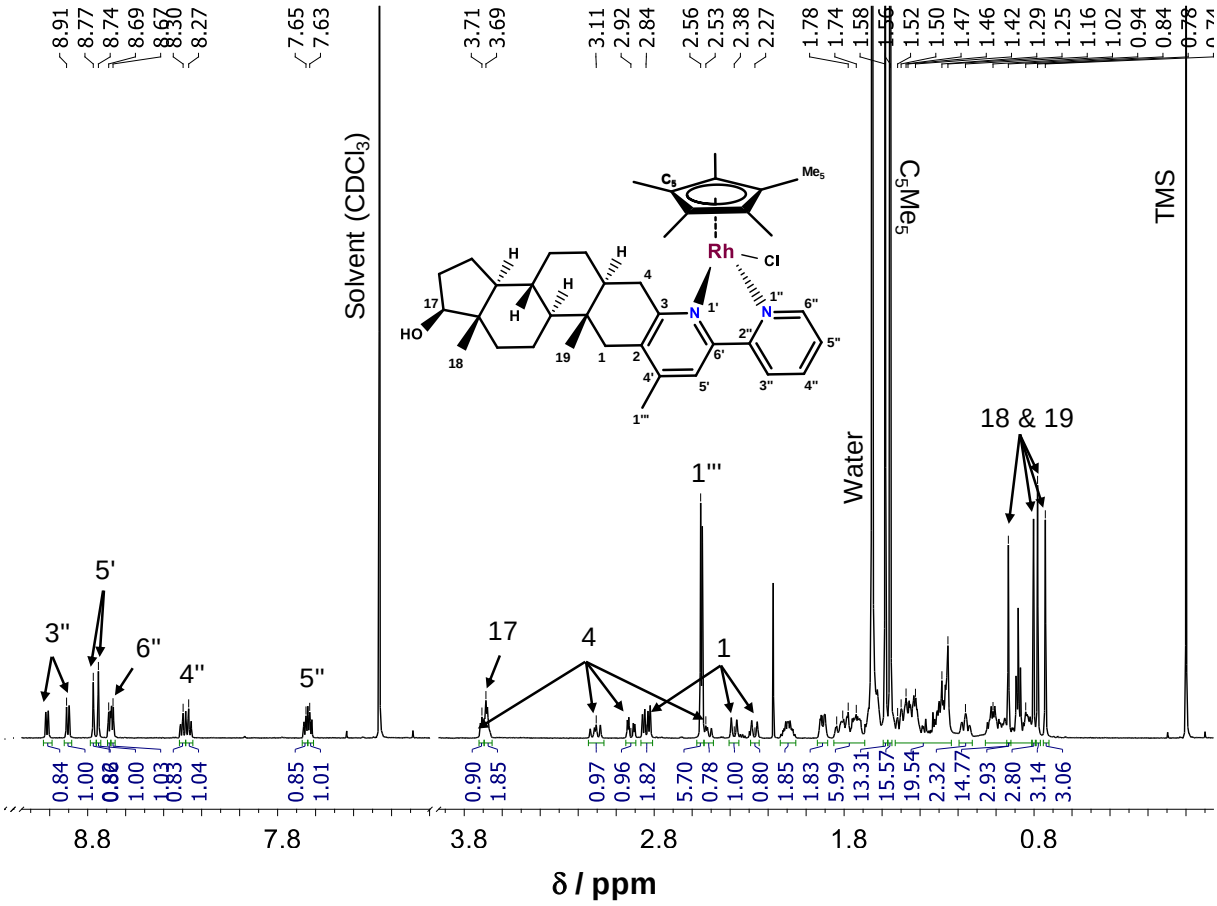

Figure S1. ^{1}H NMR spectrum of [RhCp*(4-Me-bpy-St-OH)Cl]Cl (**1**) in $CDCl_3$. Inserted structure shows the numbering of peaks.

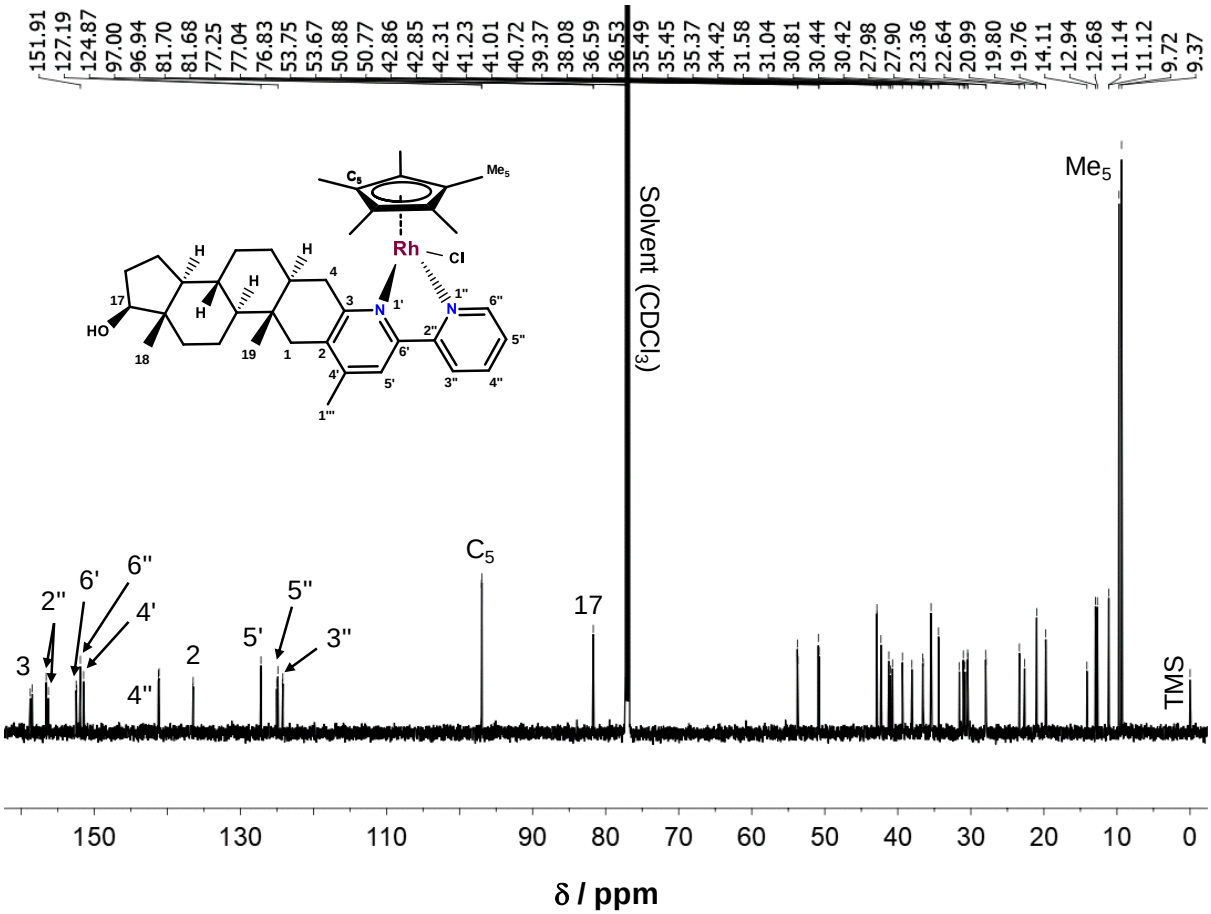

Figure S2. ^{13}C NMR spectrum of [RhCp*(4-Me-bpy-St-OH)Cl]Cl (**1**) in $CDCl_3$. Inserted structure shows the numbering of peaks.

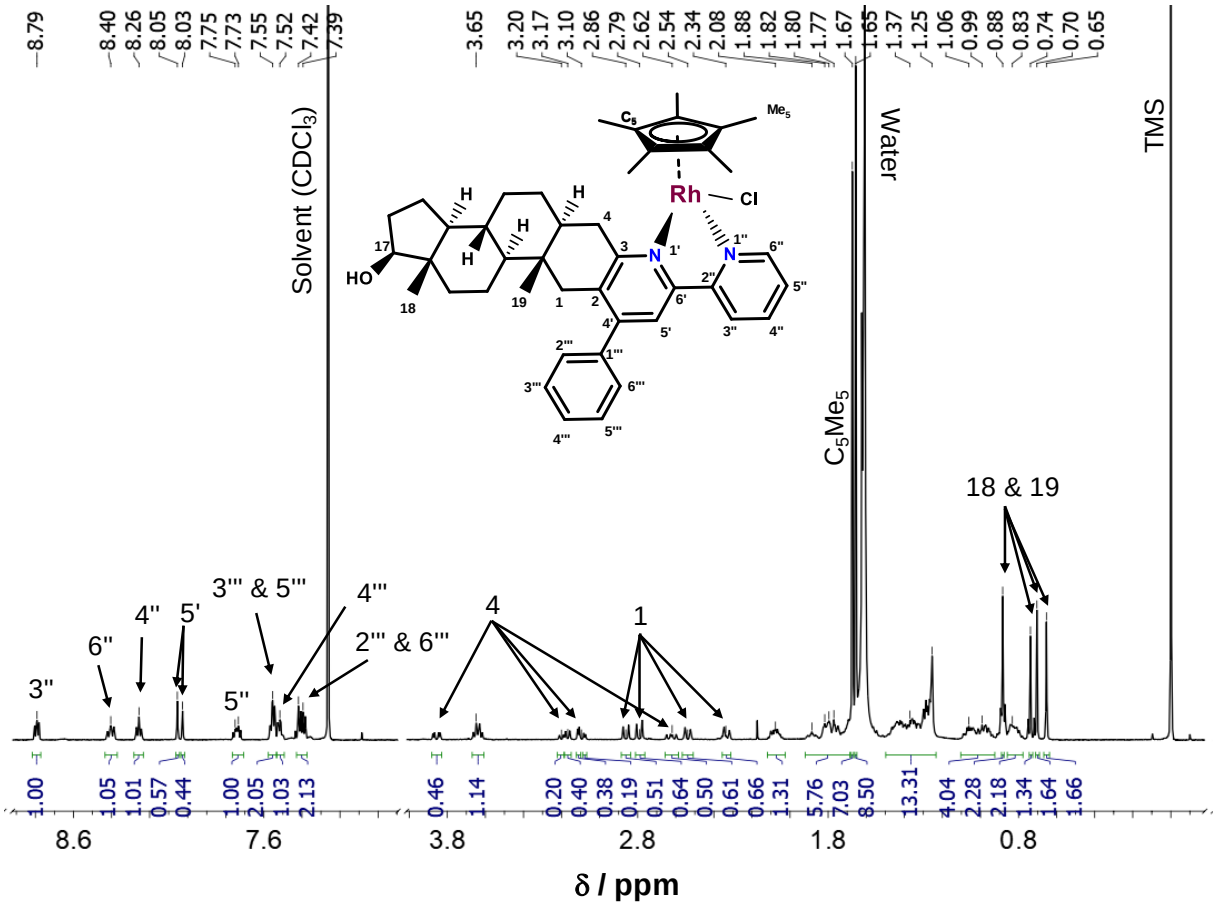

Figure S3. ^{1}H NMR spectrum of [RhCp*(4-Ph-bpy-St-OH)Cl]Cl (**2**) in $CDCl_3$. Inserted structure shows the numbering of peaks.

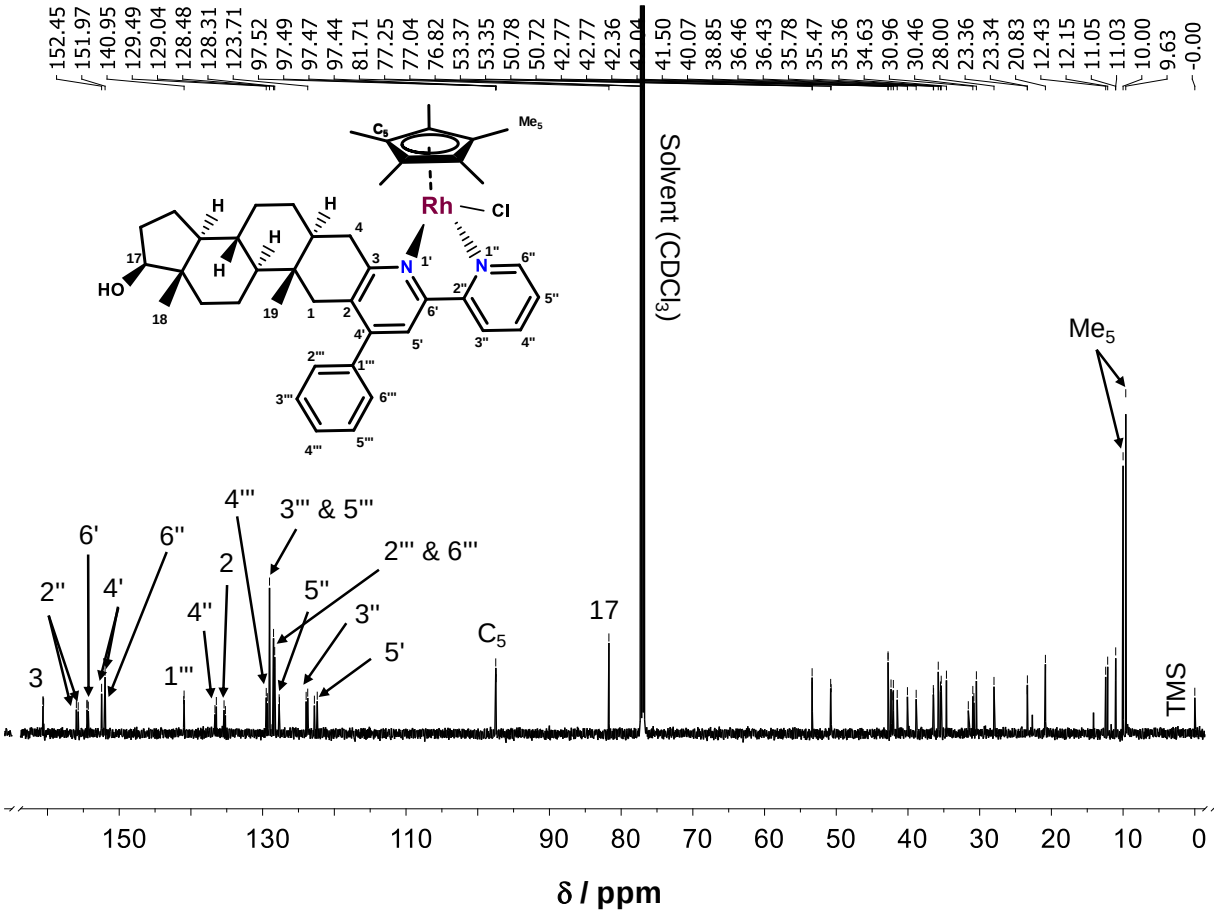

Figure S4. ^{13}C NMR spectrum of [RhCp*(4-Ph-bpy-St-OH)Cl]Cl (**2**) in $CDCl_3$. Inserted structure shows the numbering of peaks.

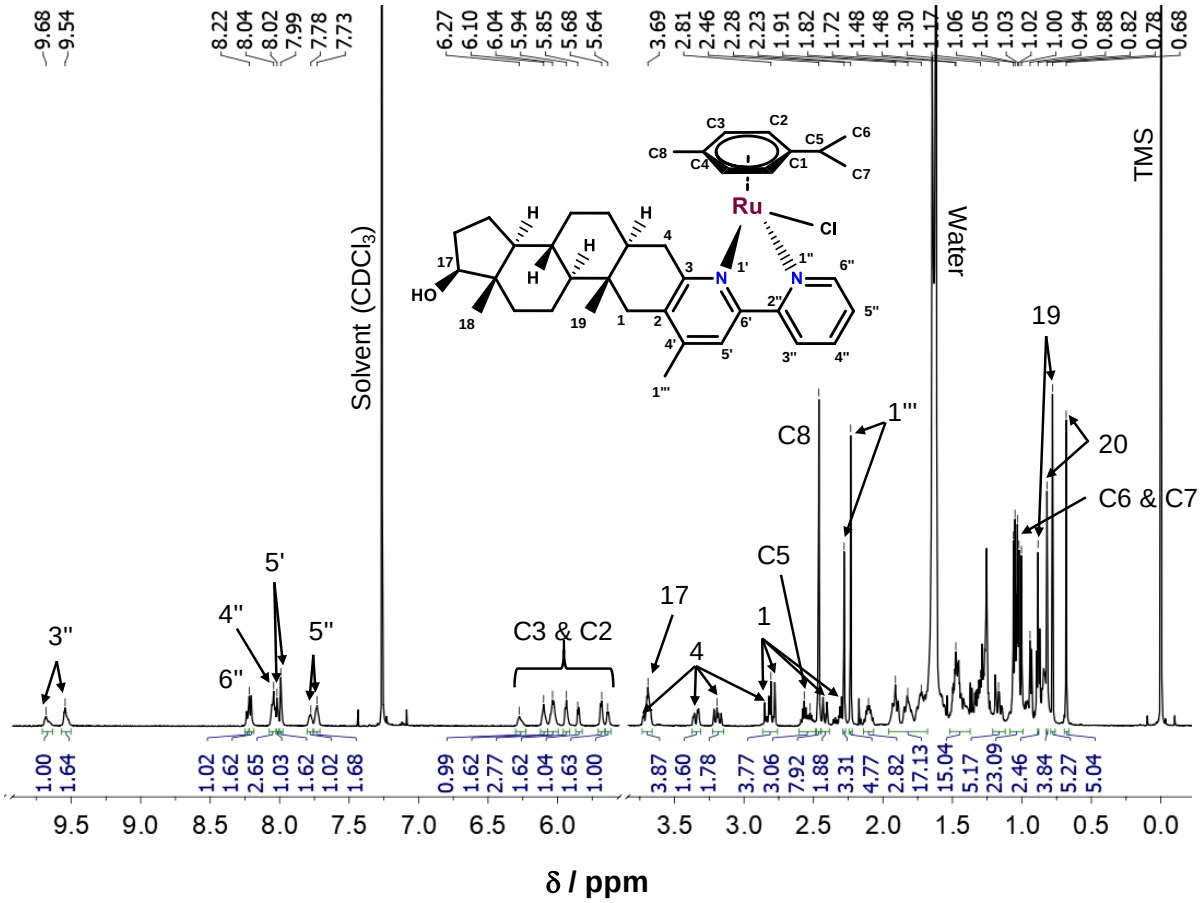

Figure S5. ^{1}H NMR spectrum of [RuCym(4-Me-bpy-St-OH)Cl]Cl (**3**) in $CDCl_3$. Inserted structure shows the numbering of peaks.

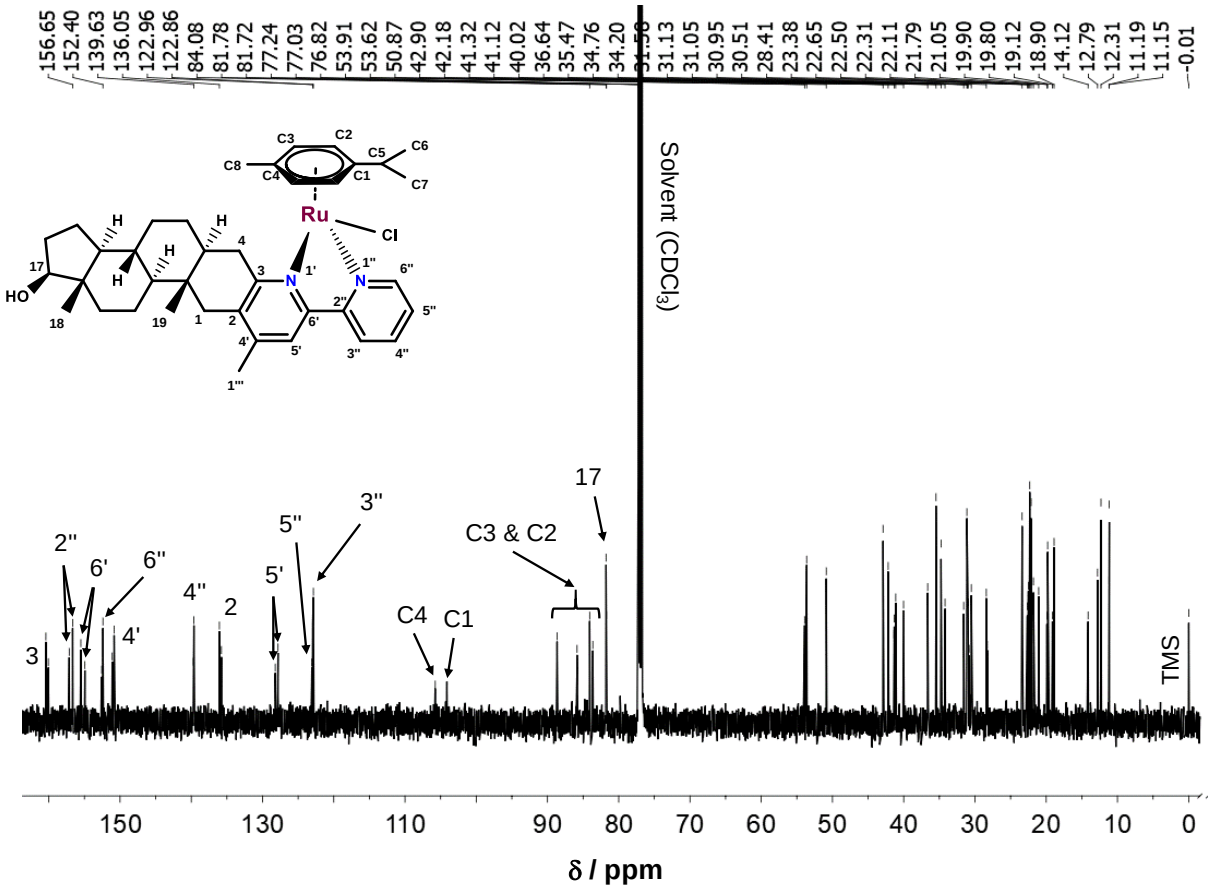

Figure S6. ^{13}C NMR spectrum of [RuCym(4-Me-bpy-St-OH)Cl]Cl (**3**) in $CDCl_3$. Inserted structure shows the numbering of peaks.

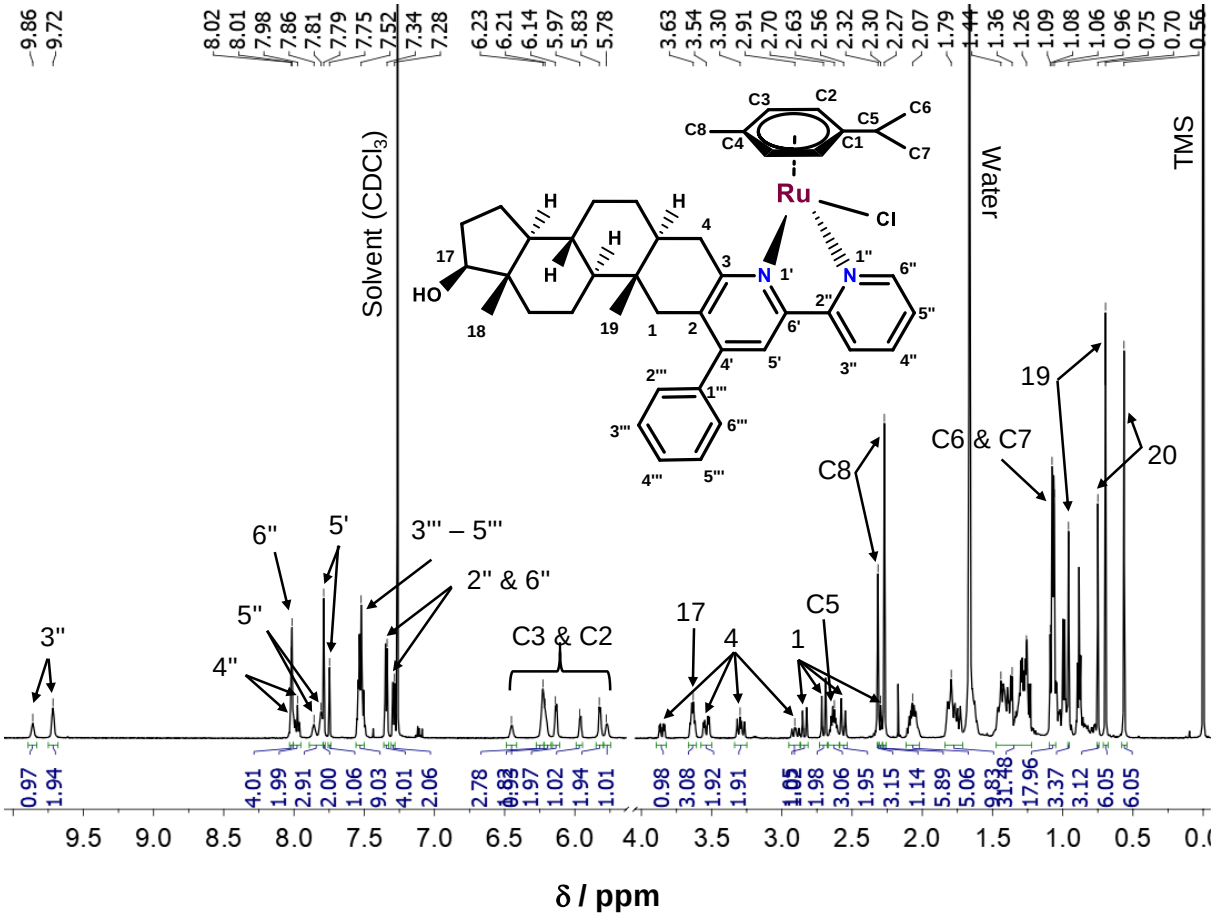

Figure S7. ^{1}H NMR spectrum of [RuCym(4-Ph-bpy-St-OH)Cl]Cl (**4**) in $CDCl_3$. Inserted structure shows the numbering of peaks.

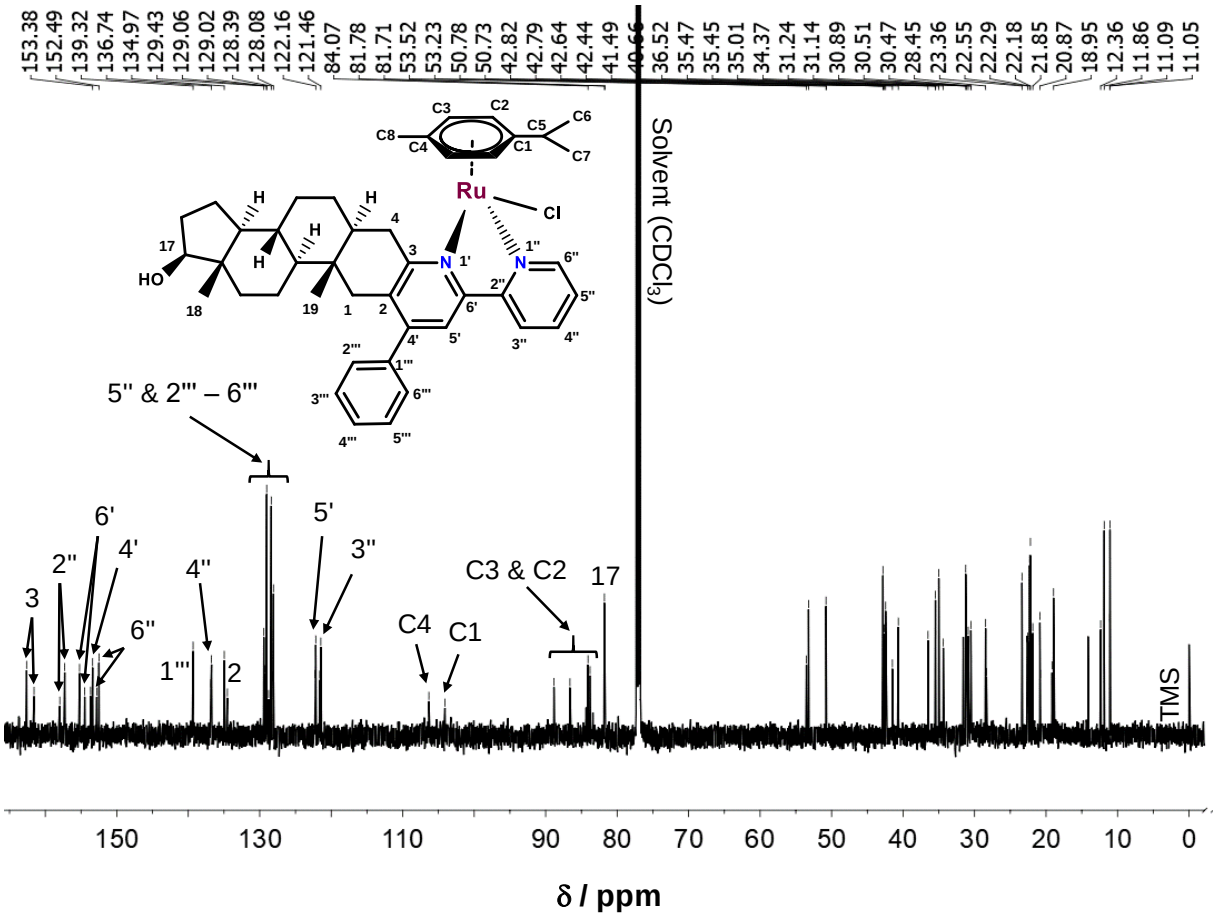

Figure S8. ^{13}C NMR spectrum of [RuCym(4-Ph-bpy-St-OH)Cl]Cl (**4**) in $CDCl_3$. Inserted structure shows the numbering of peaks.

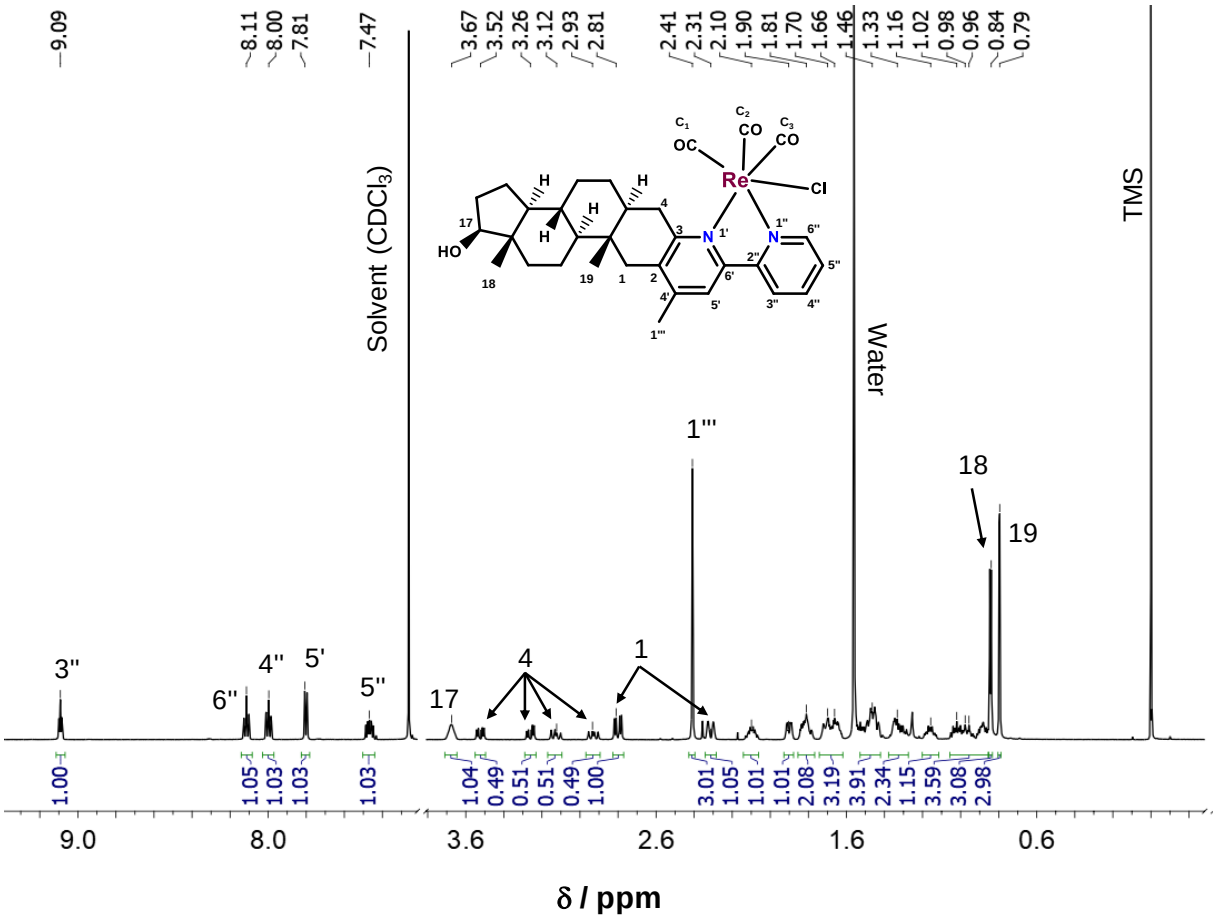

Figure S9. ^{1}H NMR spectrum of [Re(CO_3)(4-Me-bpy-St-OH)Cl] (**5**) in $CDCl_3$. Inserted structure shows the numbering of peaks.

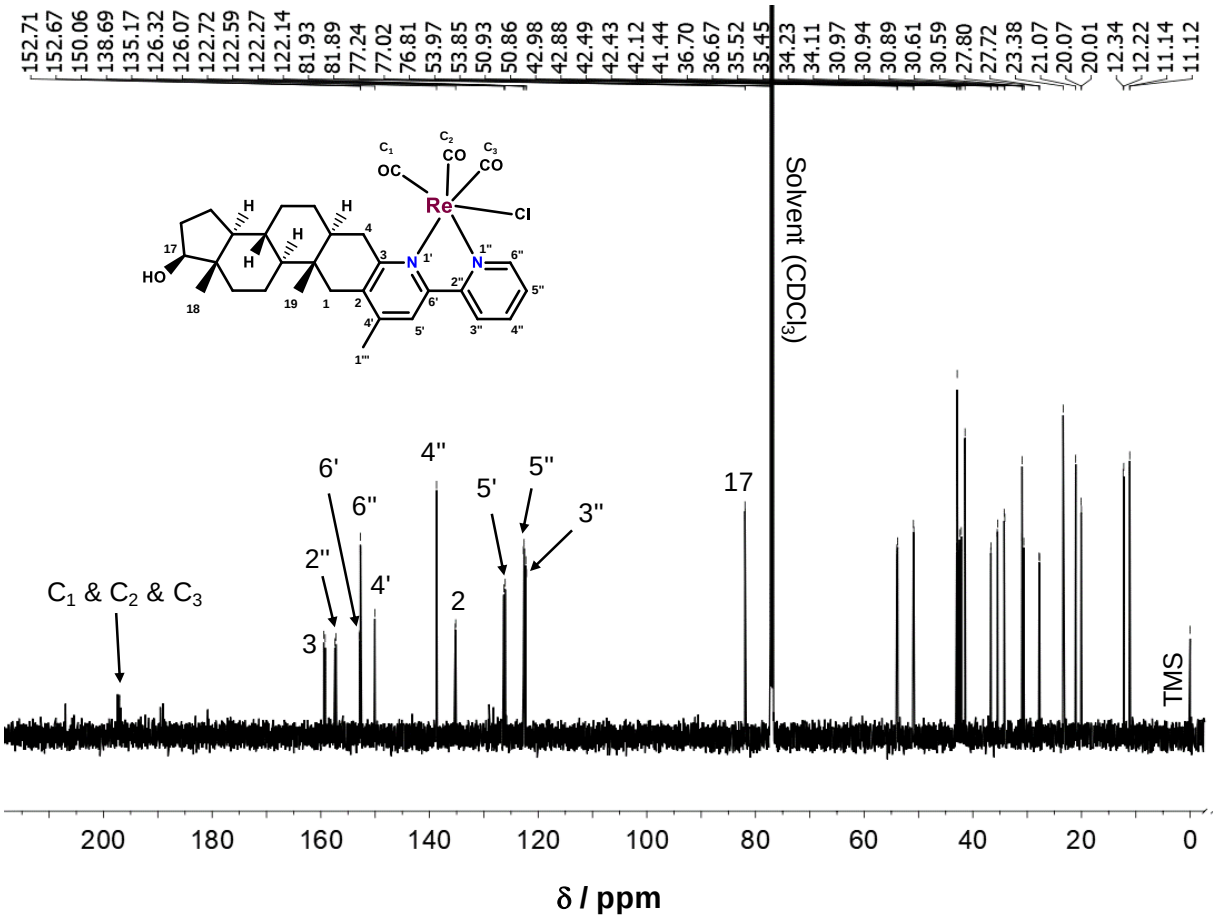

Figure S10. ^{13}C NMR spectrum of [Re(CO_3)(4-Me-bpy-St-OH)Cl] (**5**) in $CDCl_3$. Inserted structure shows the numbering of peaks.

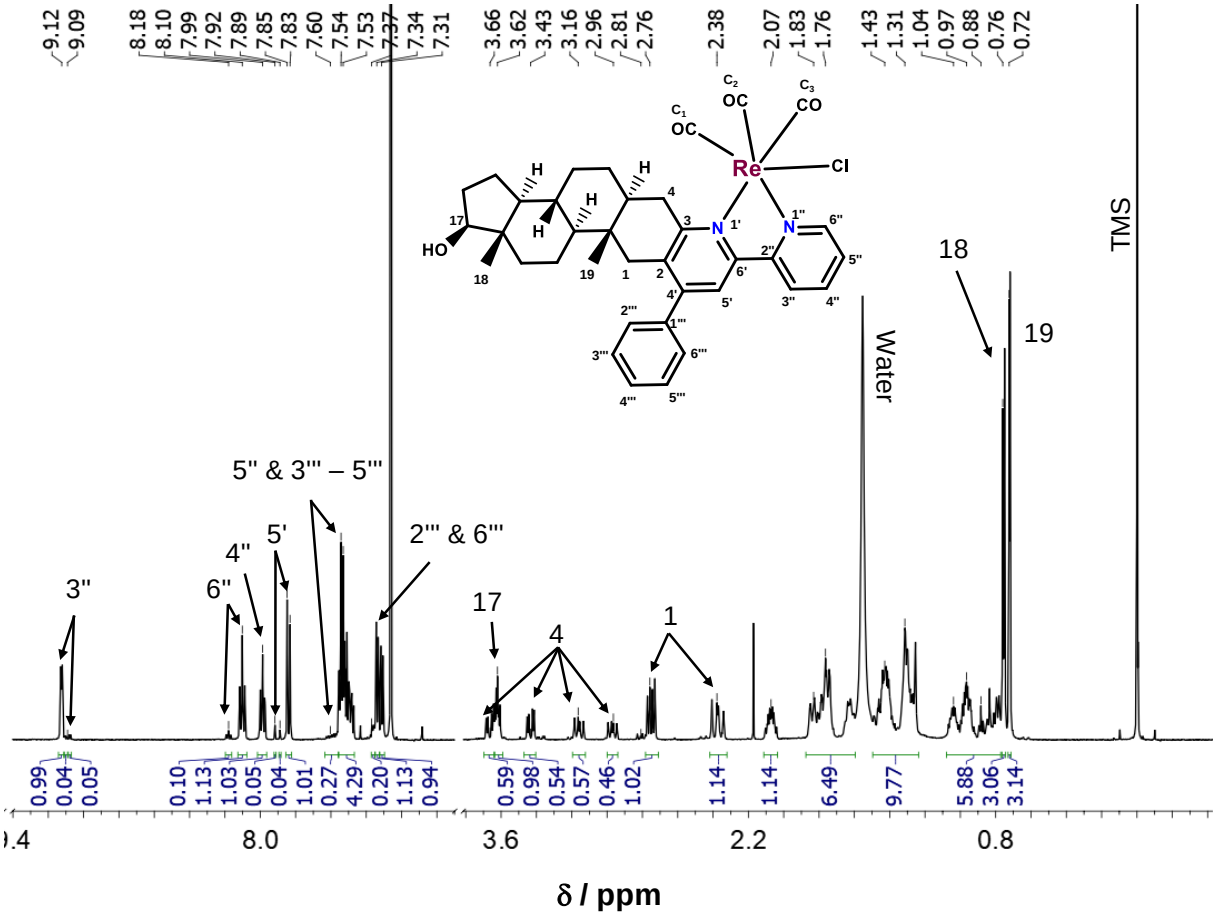

Figure S11. ^{1}H NMR spectrum of [Re(CO_3)(4-Ph-bpy-St-OH)Cl] (**6**) in $CDCl_3$. Inserted structure shows the numbering of peaks.

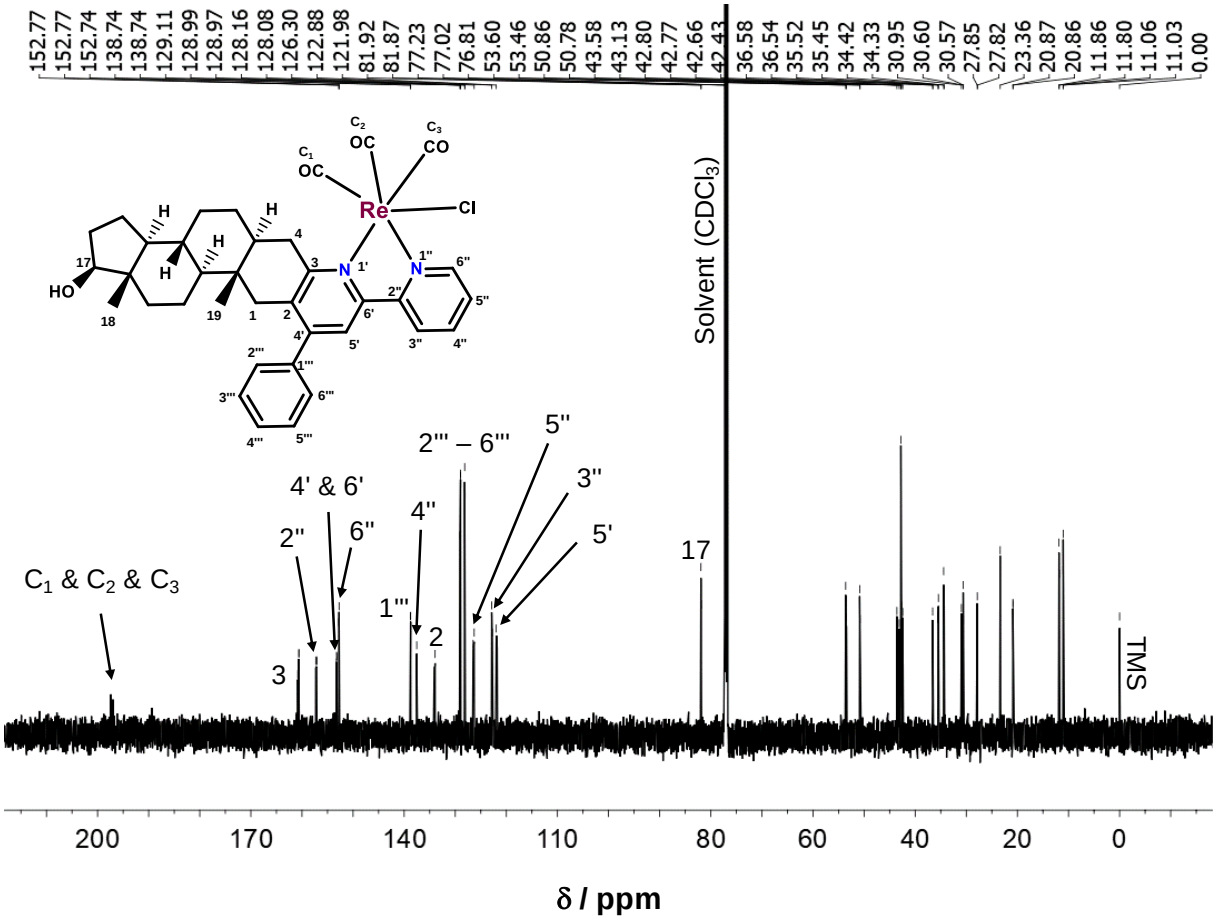

Figure S12. ^{13}C NMR spectrum of [Re(CO_3)(4-Ph-bpy-St-OH)Cl] (**6**) in $CDCl_3$. Inserted structure shows the numbering of peaks.

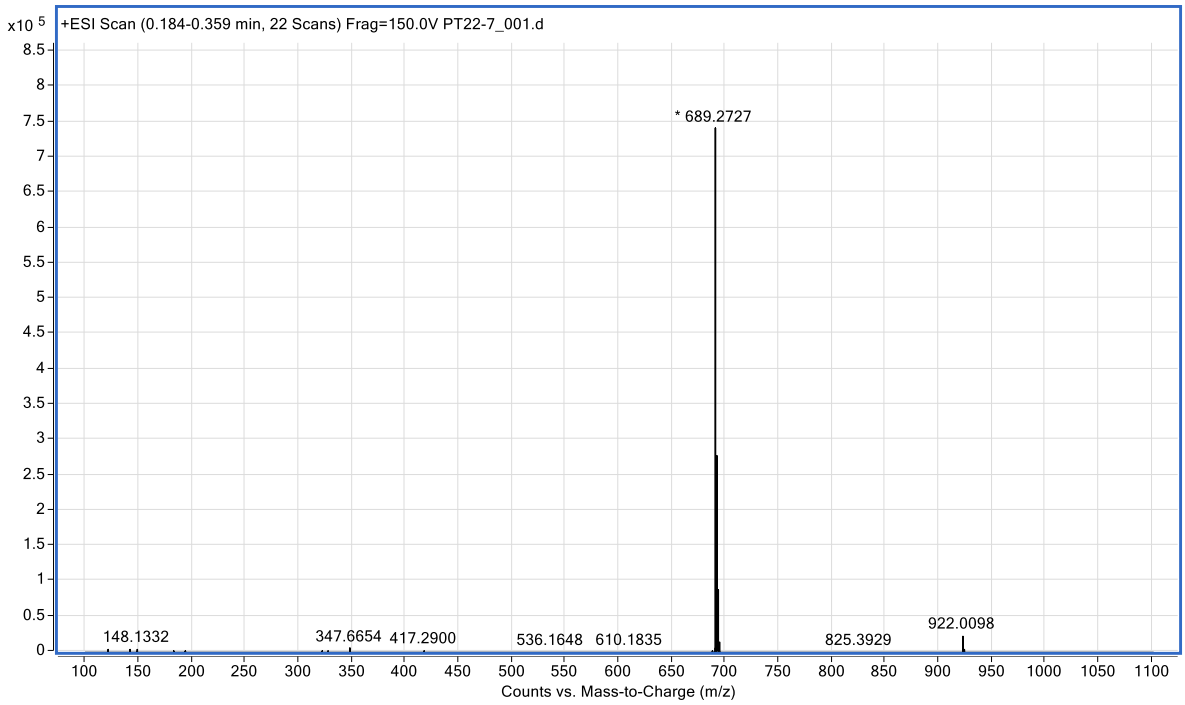

Figure S13. High resolution electrospray ionization MS (HR-ESI-MS) spectrum of [RhCp*(4-Me-bpy-St-OH)Cl]Cl (**1**) recorded in CH_3CN.

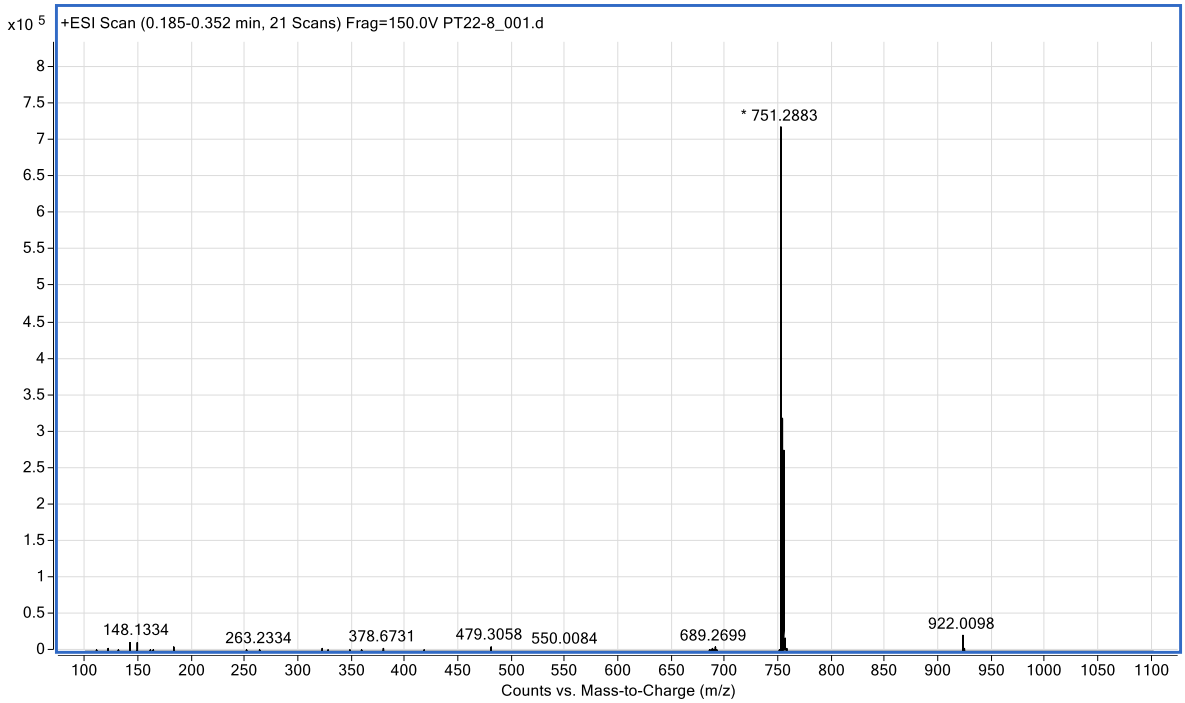

Figure S14. High resolution electrospray ionization MS (HR-ESI-MS) spectrum of [RhCp*(4-Ph-bpy-St-OH)Cl]Cl (**2**) recorded in CH_3CN.

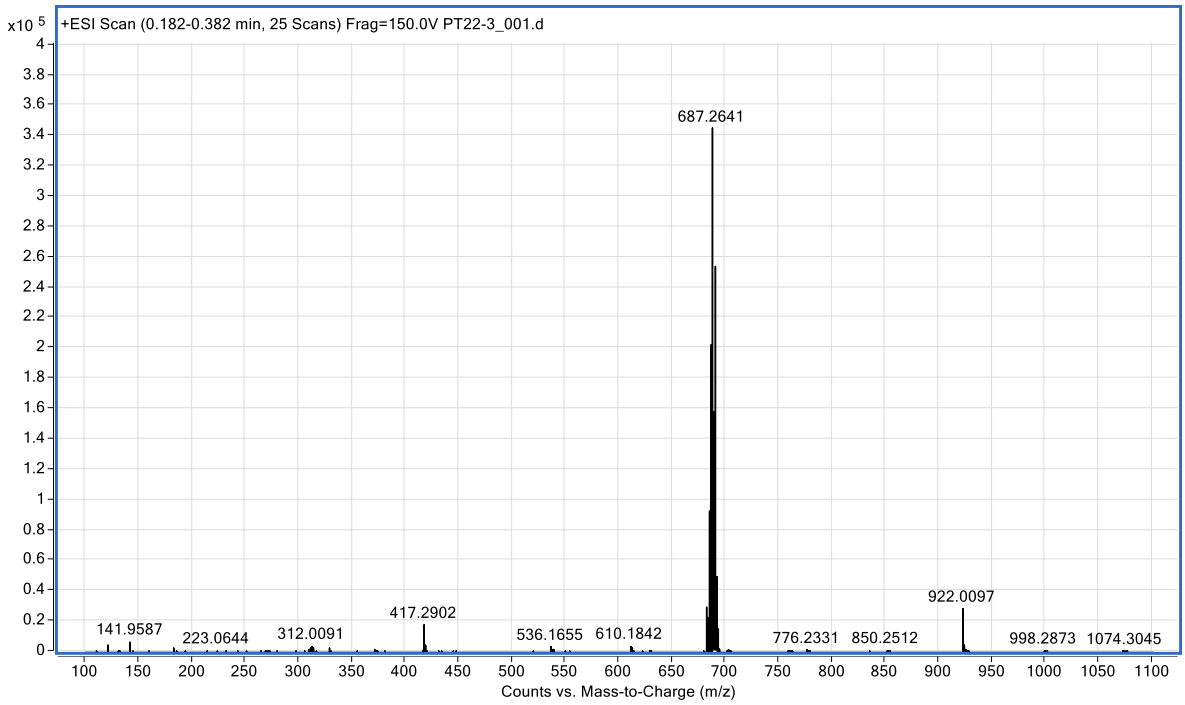

Figure S15. High resolution electrospray ionization MS (HR-ESI-MS) spectrum of [RuCym(4-Me-bpy-St-OH)Cl]Cl (**3**) recorded in CH_3CN.

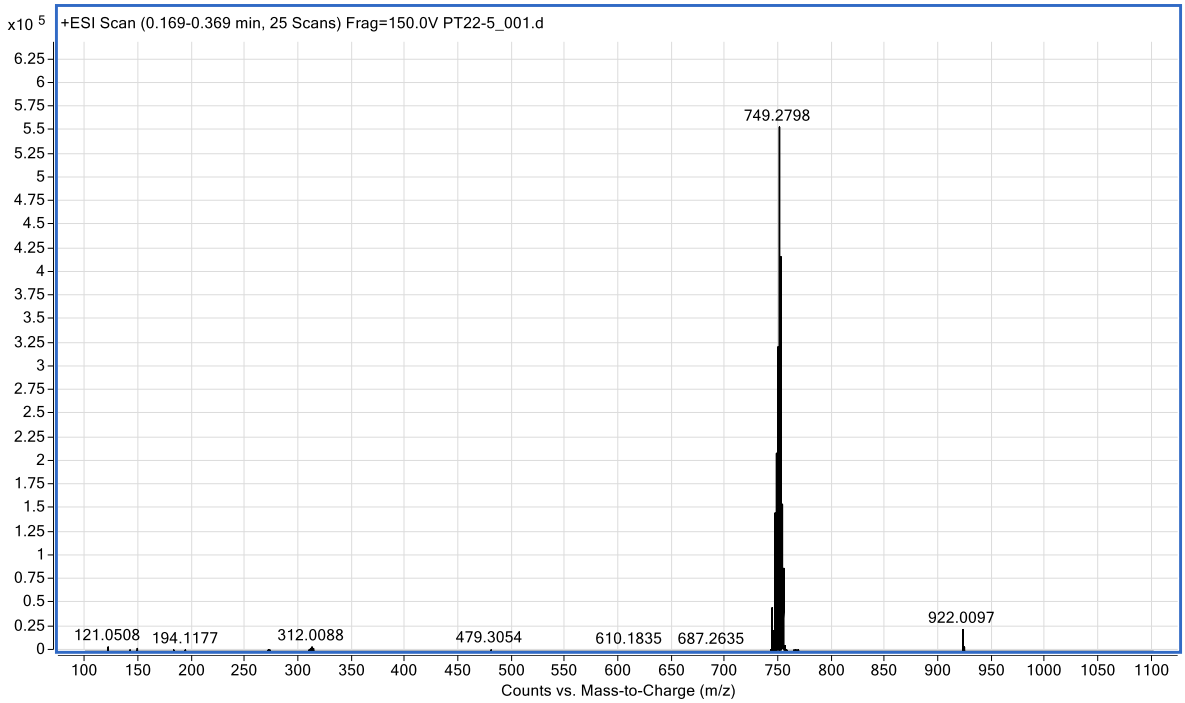

Figure S16. High resolution electrospray ionization MS (HR-ESI-MS) spectrum of [RuCym(4-Ph-bpy-St-OH)Cl]Cl (**4**) recorded in CH_3CN.

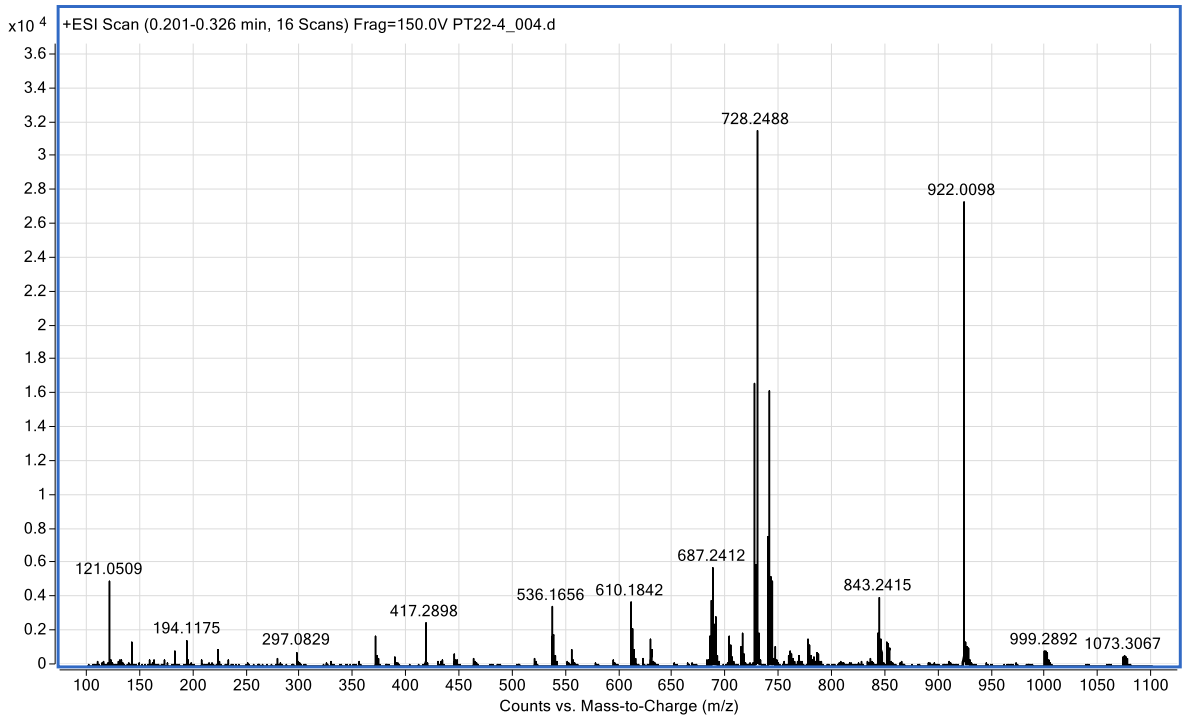

Figure S17. High resolution electrospray ionization MS (HR-ESI-MS) spectrum of [Re(CO_3)(4-Me-bpy-St-OH)Cl] (**5**) recorded in CH_3CN.

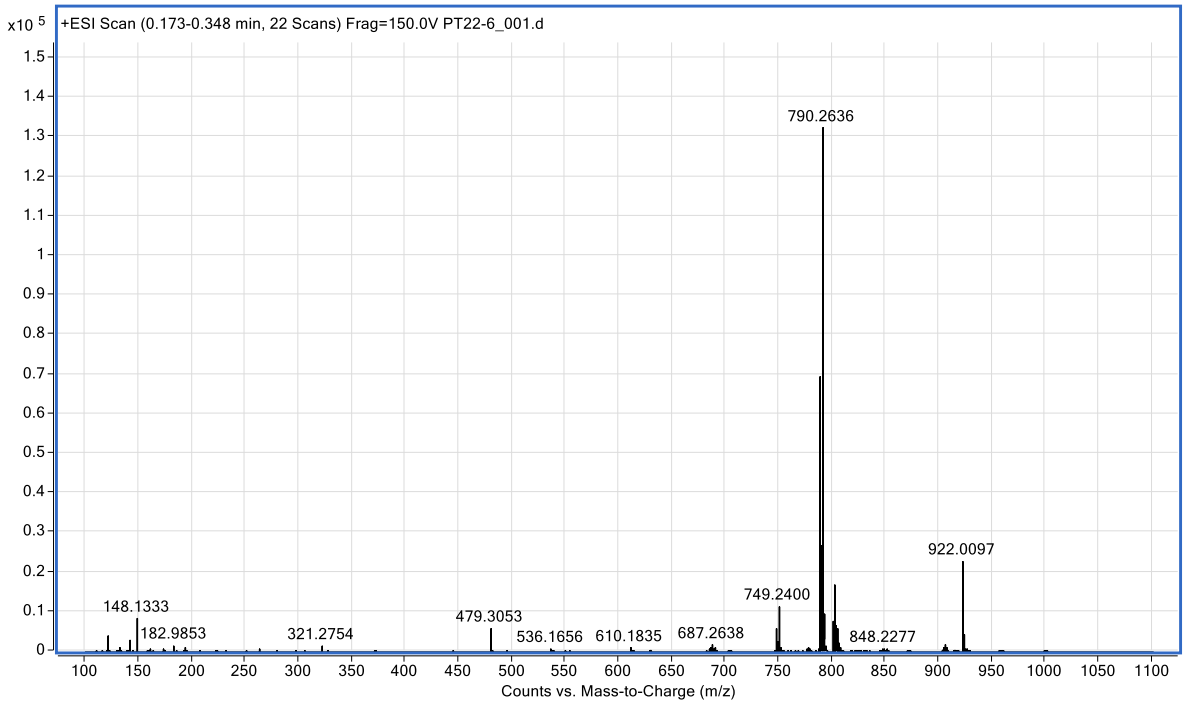

Figure S18. High resolution electrospray ionization MS (HR-ESI-MS) spectrum of [Re(CO_3)(4-Ph-bpy-St-OH)Cl] (**6**) recorded in CH_3CN.

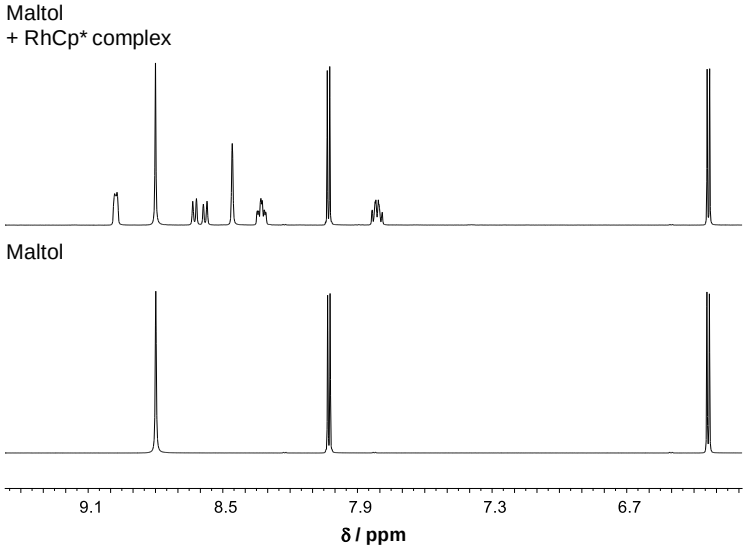

Figure S19. Quantitative-NMR: ^{1}H NMR spectrum of maltol and [RhCp*(4-Me-bpy-St-OH)Cl]Cl (**1**) complex together with maltol in DMSO-d_6. Based on the integrals the RhCp* complex is found with 2 chloride ions and 4 water molecules.

Figure S20. Photograph of the analysed crystal of complex [Re(CO)$_3$(4-Me-bpy-St-OH)Cl] (**5**).

Table S1. log*D* values at pH = 7.40 and pK_a values[a] of the (*N,O*) ligands along with the determined IC_{50} values (expressed in µM) in human cancerous cell lines.

		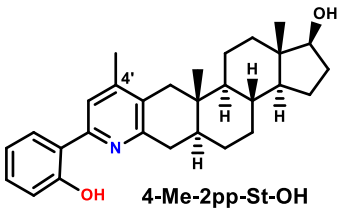 4-Me-2pp-St-OH	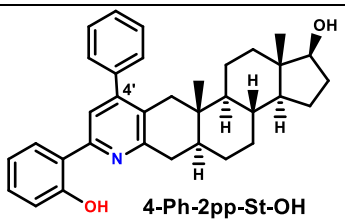 4-Ph-2pp-St-OH
log$D_{7.40}$		+ 3.01 ± 0.05	+ 3.43 ± 0.25
pK_{a1}: $N1'_{2pp}H^+$		5.21[a]	8.54[a]
pK_{a2}: OH_{phenol}		4.49[a]	8.52[a]
IC_{50} / µM	LNCaP	>100	>100
	PC3	>100	>100
	MCF-7	8.7 ± 0.8	15.2 ± 0.2
	Colo205	3.9 ± 0.1	9.5 ± 0.4

[a] As precipitation was also observed even at higher DMSO content (60% (v/v) DMSO/H2O), UV-vis or ^{1}H NMR titrations could not be performed, the pK_a values were predicted by the Marvin software of ChemAxon.[SI1]

Reference SI1: ChemAxon, Ltd. Instant J. Chem. / MarwinSketch; ChemAxon Ltd.: Budapest, Hungary, 2012.

Table S2. Crystallographic data for complex $[Re(CO)_3(4\text{-Me-bpy-St-OH})Cl]$ (**5**).

Complex	(**5**)
CCDC No.	2302275
Empirical formula	$C_{31}H_{36}ClN_2O_4Re$
Formula weight	722.27
Temperature [K]	150.00(10)
Crystal system	triclinic
Space group	P1
a [Å]	8.9975(3)
b [Å]	12.9898(4)
c [Å]	13.9898(5)
α [°]	110.232(3)
β [°]	107.742(3)
γ [°]	91.611(3)
Volume [$Å^3$]	1444.82(9)
Z	2
ρ_{calc} [g cm^{-3}]	1.660
μ [mm^{-1}]	4.336
F(000)	720.0
Crystal size [mm^3]	0.1 × 0.08 × 0.02
Radiation	Mo Kα (λ = 0.71073)
2Θ range for data collection [°]	4.802 to 58.912
Index ranges	$-12 \leq h \leq 12$, $-17 \leq k \leq 17$, $-19 \leq l \leq 19$
Reflections collected	20202
Independent reflections	12182 [R_{int} = 0.0378, R_{sigma} = 0.0656]
Data/restraints/parameters	12182/3/651
Goodness-of-fit on F^2	0.975
Final R indexes [I ≥ 2σ (I)]	R_1 = 0.0320, wR_2 = 0.0578
Final R indexes [all data]	R_1 = 0.0416, wR_2 = 0.060
Largest diff. peak / hole [e $Å^{-3}$]	1.26/-1.35
Flack parameter	-0.036(9)

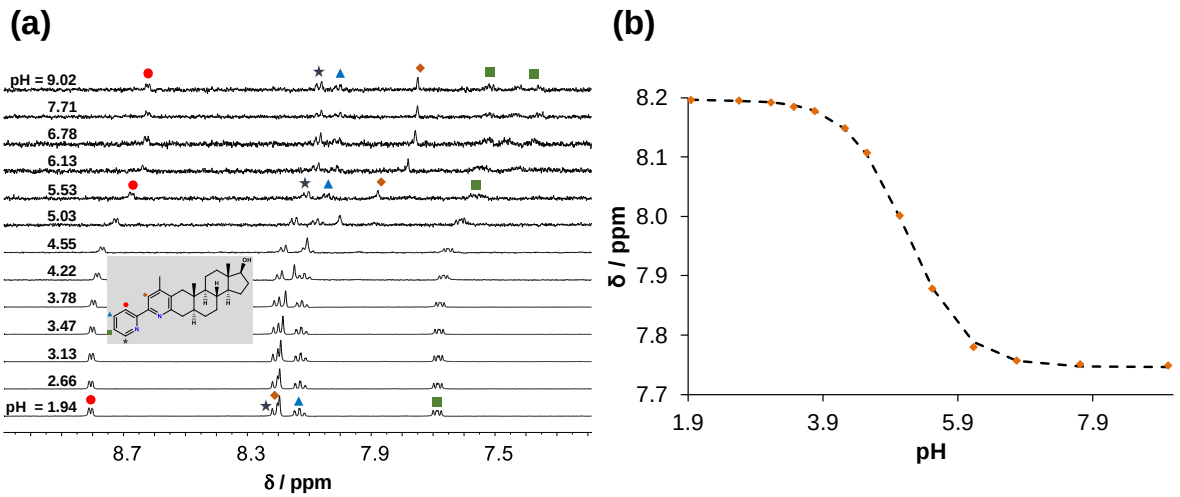

Figure S21. (a) ^{1}H NMR spectra of 4-Me-bpy-St-OH in the low-field region at different pH values, and (b) chemical shift values of the C(5')H proton (♦) along with the fitted (dashed) line. {c_{ligand} = 680 μM, I = 0.10 M KCl, 30% (v/v) DMSO-d_6/H_2O}

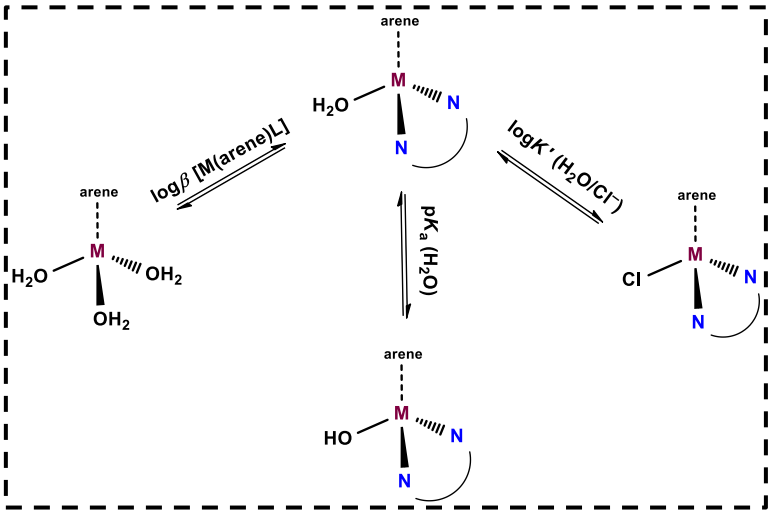

Scheme S1. Solution equilibrium processes occurring in the solution of the half-sandwich RuCym and RhCp* complexes.

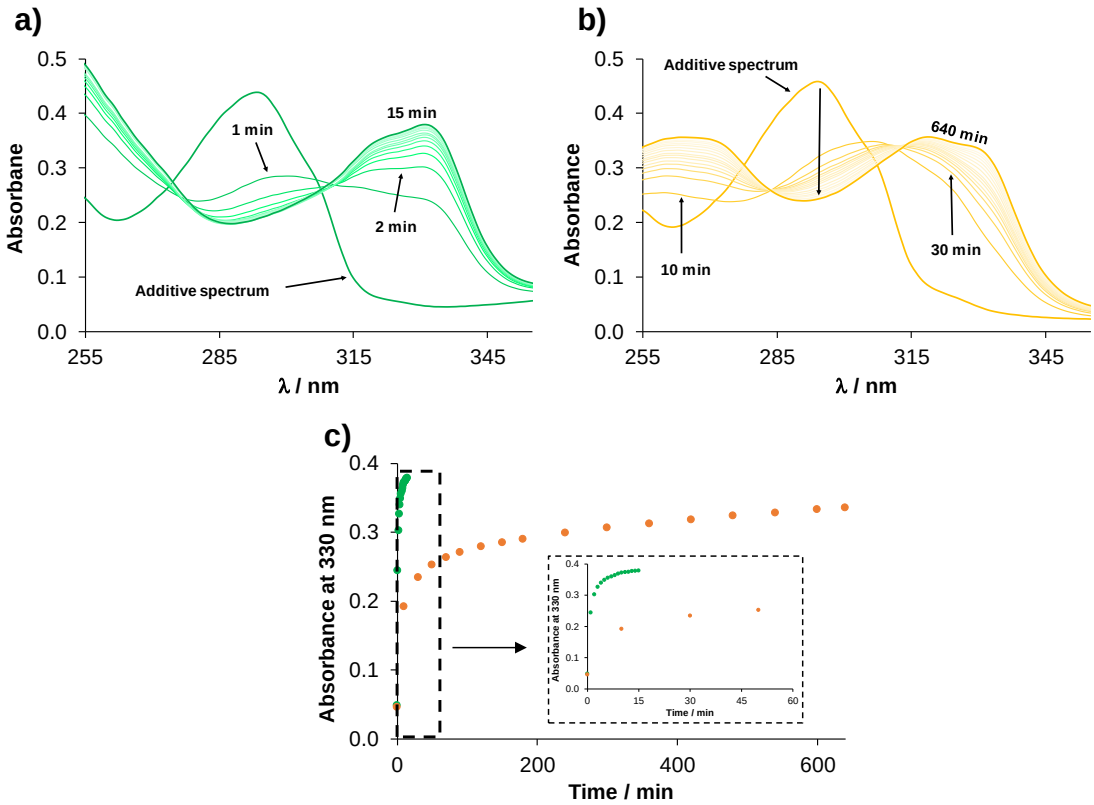

Figure S22. Complex formation process in time for (a) RhCp* – 4-Me-bpy-St-OH and (b) RuCym – 4-Me-bpy-St-OH (1:1) systems at pH = 4.0 followed by UV-vis spectrophotometry. (c) Absorbance values at 330 nm as a function of time: RhCp* (●), RuCym (●). {$c_{RuCym/RhCp*} = c_{ligand}$ = 30 μM, T = 25.0 °C, ℓ = 1 cm, 30% (v/v) DMSO/H_2O}

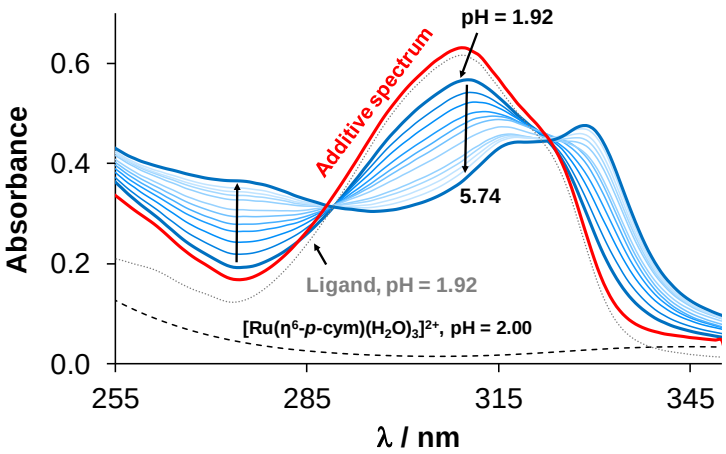

Figure S23. UV-vis spectra of the RuCym – 4-Me-bpy-St-OH (1:1) system at various pH values (1.92 → 5.74). The spectrum of the organometallic triaqua cation (black dashed line), ligand (grey dotted line) and their additive spectrum (red solid line) are also indicated. Notably, the aqua co-ligands are replaced partly by chlorido ligands in the presence of chloride ions. {$c_{RuCym} = c_{ligand}$ = 30 μM, I = 0.10 M KCl, T = 25.0 °C, ℓ = 1 cm, 30 % (v/v) DMSO/water}

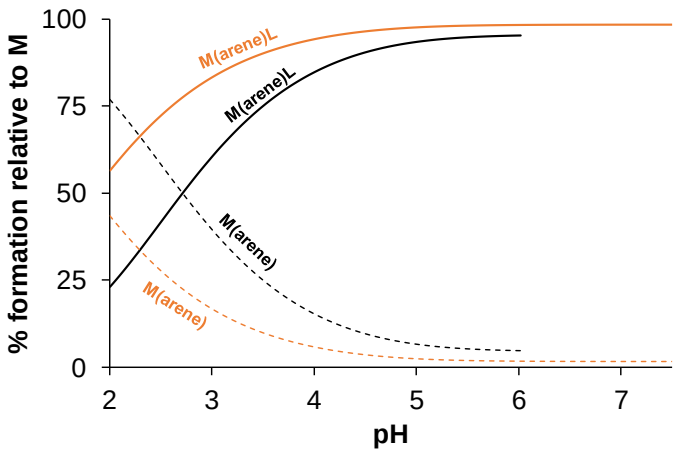

Figure S24. Concentration distribution curves calculated for the RhCp* – 4-Me-bpy-St-OH (orange, solid and dashed lines) and for the RuCym – 4-Me-bpy-St-OH (black, solid and dashed lines) (1:1) systems. {$c_{ligand} = c_{RhCp*/RuCym}$ = 30 µM, I = 0.10 M KCl, T = 25.0 °C, 30% (v/v) DMSO/H_2O}

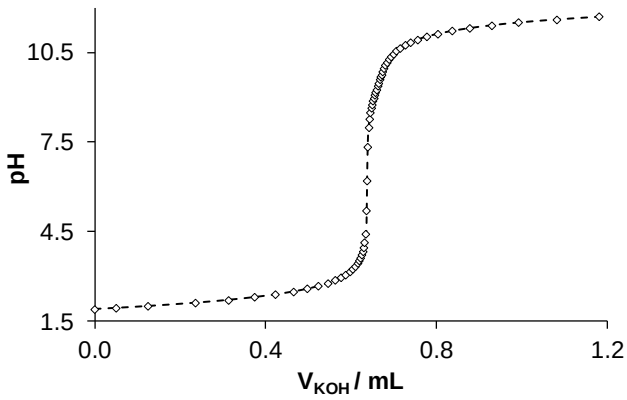

Figure S25. pH-potentiometric titration curve of the [RhCp*(4-Me-bpy-St-OH)Cl]Cl complex (**1**) (◊) along with the fitted (dashed) line {$c_{complex}$ = 660 µM, I = 0.20 M KNO_3, T = 25.0 °C}

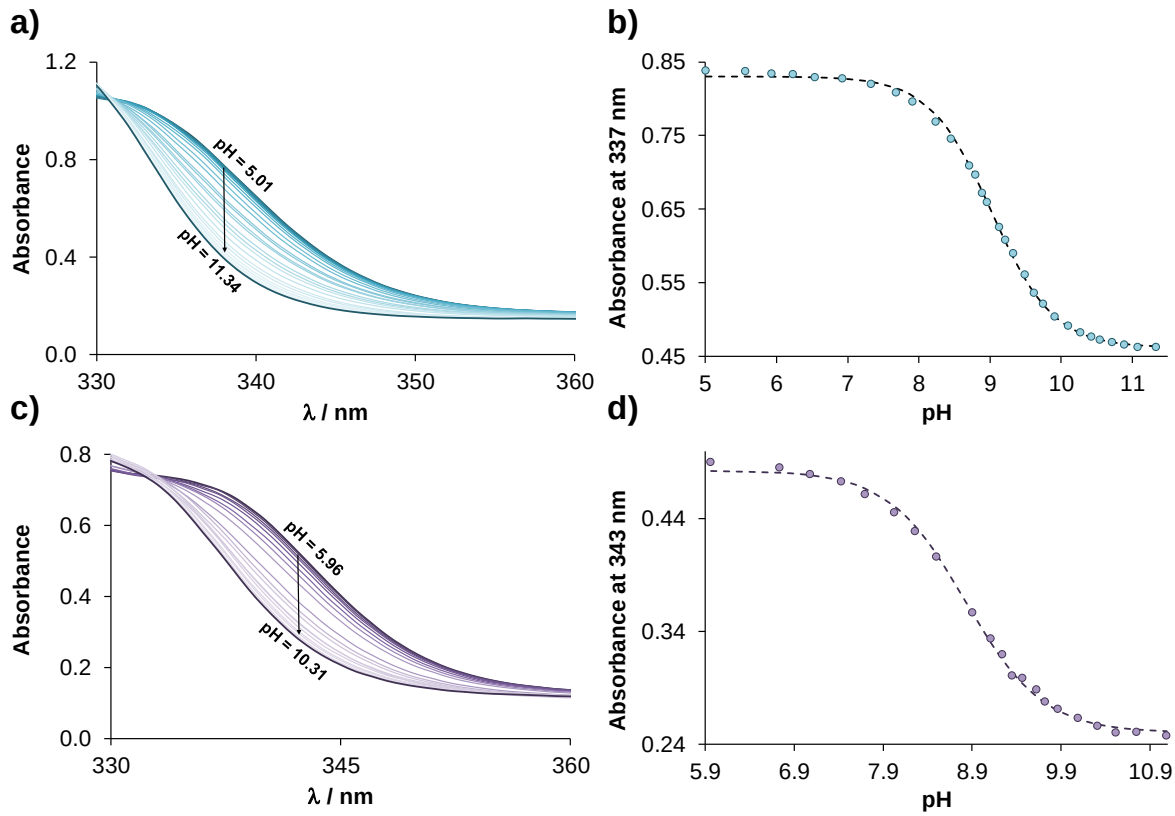

Figure S26. (a) UV-vis spectra of the [RhCp*(4-Me-bpy-St-OH)Cl]Cl complex (**1**) at various pH values (5.01 → 11.34). (b) Absorbance values at 337 nm (○) as a function of pH together with the fitted curve. {$c_{(1)}$ = 158 μM, I = 0.20 M KNO_3, T = 25.0 °C, ℓ = 1 cm} (c) UV-vis spectra of the [RhCp*(4-Ph-bpy-St-OH)Cl]Cl complex (**2**) at various pH values (5.96 → 10.31). (d) Absorbance values at 343 nm for the same complex as a function of pH. {$c_{(2)}$ = 103 μM, I = 0.20 M KNO_3, T = 25.0 °C, ℓ = 1 cm}

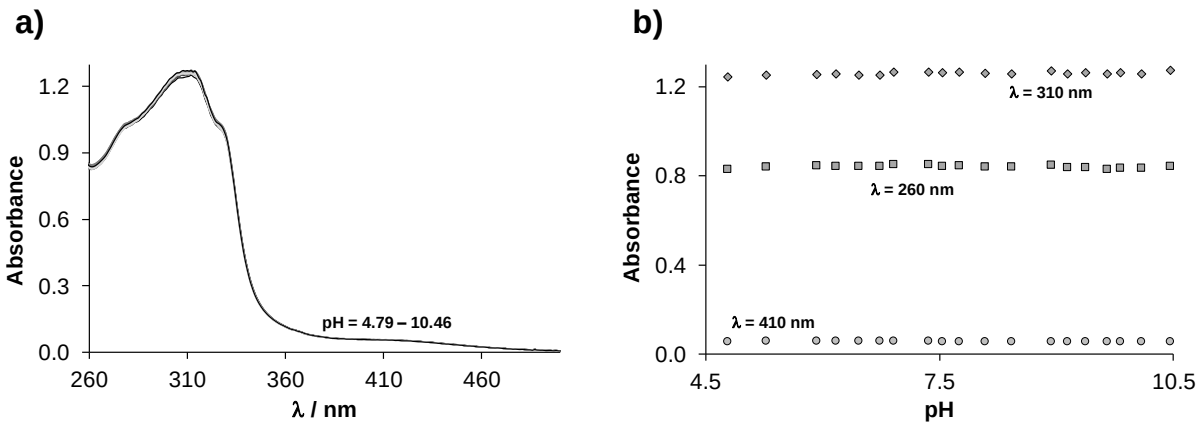

Figure S27. (a) UV–vis spectra of the [RuCym(4-Me-bpy-St-OH)Cl]Cl complex (**3**) at various pH values (4.79 → 10.36). (b) Absorbance values at different wavelengths as a function of pH. {$c_{(3)}$ = 123 μM, I = 0.20 M KNO_3, T = 25.0 °C, ℓ = 1 cm}

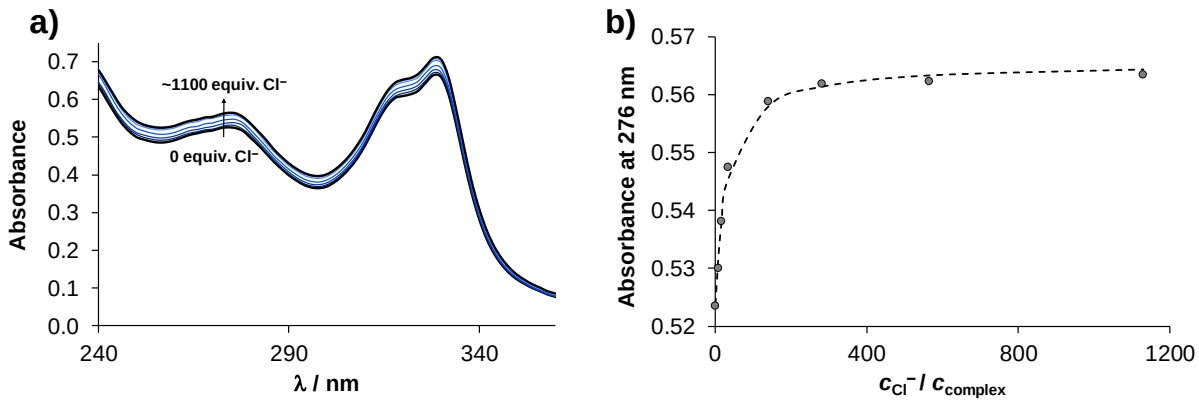

Figure S28. (a) UV-vis spectra of [RuCym(4-Me-bpy-St-OH)Cl]Cl (**3**) in the absence and presence of various equivalents of chloride ions. (b) Absorbance values at 276 nm as a function of c_{Cl-} / $c_{complex}$ ratio along with the fitted (dashed) line. {$c_{(3)}$ = 237 μM; pH = 7.40 (phosphate buffer); I = 0.20 M KNO_3; ℓ = 0.2 cm; T = 25.0 °C}

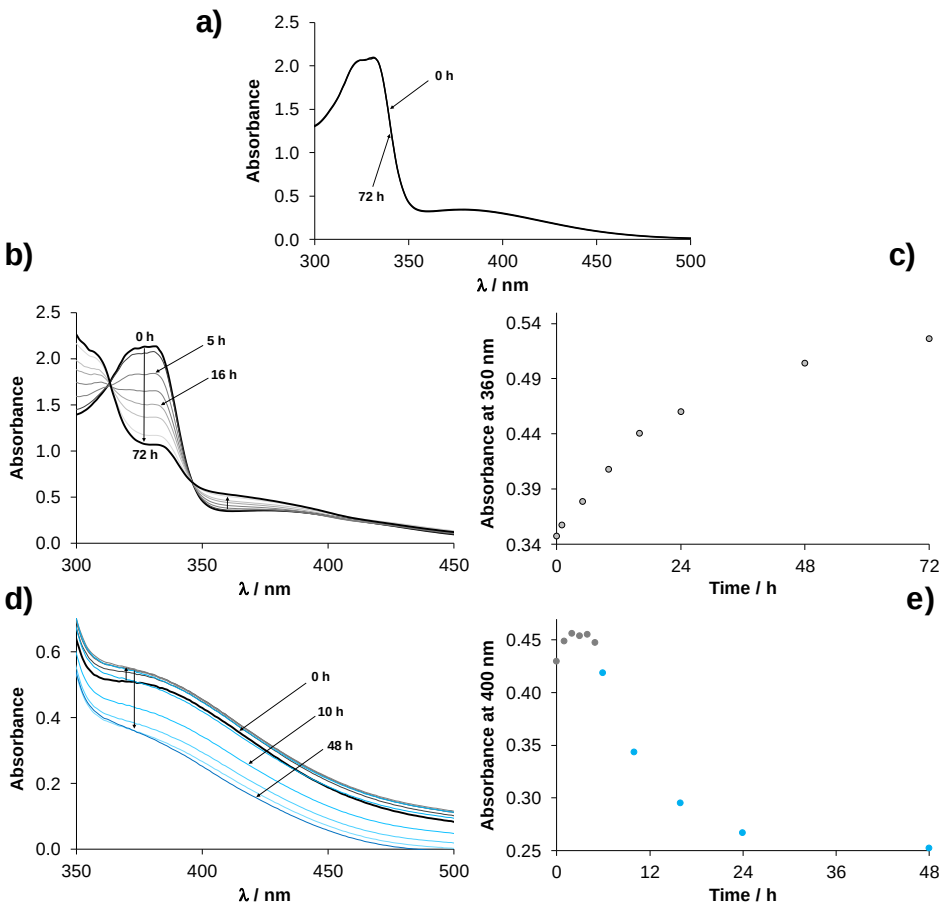

Figure S29. UV-vis spectra of the [RhCp*(4-Ph-bpy-St-OH)Cl]Cl complex (**2**) in (a) PBS' buffer (pH = 7.40), (b) RPMI-1640 biological medium and d) blood serum. Absorbance values at 360 and 400 nm as a function of time in the case of (c) RPMI-1640 and (e) blood serum. {$c_{(2)}$ = 150 μM, T = 25.0 °C, ℓ = 1 cm}

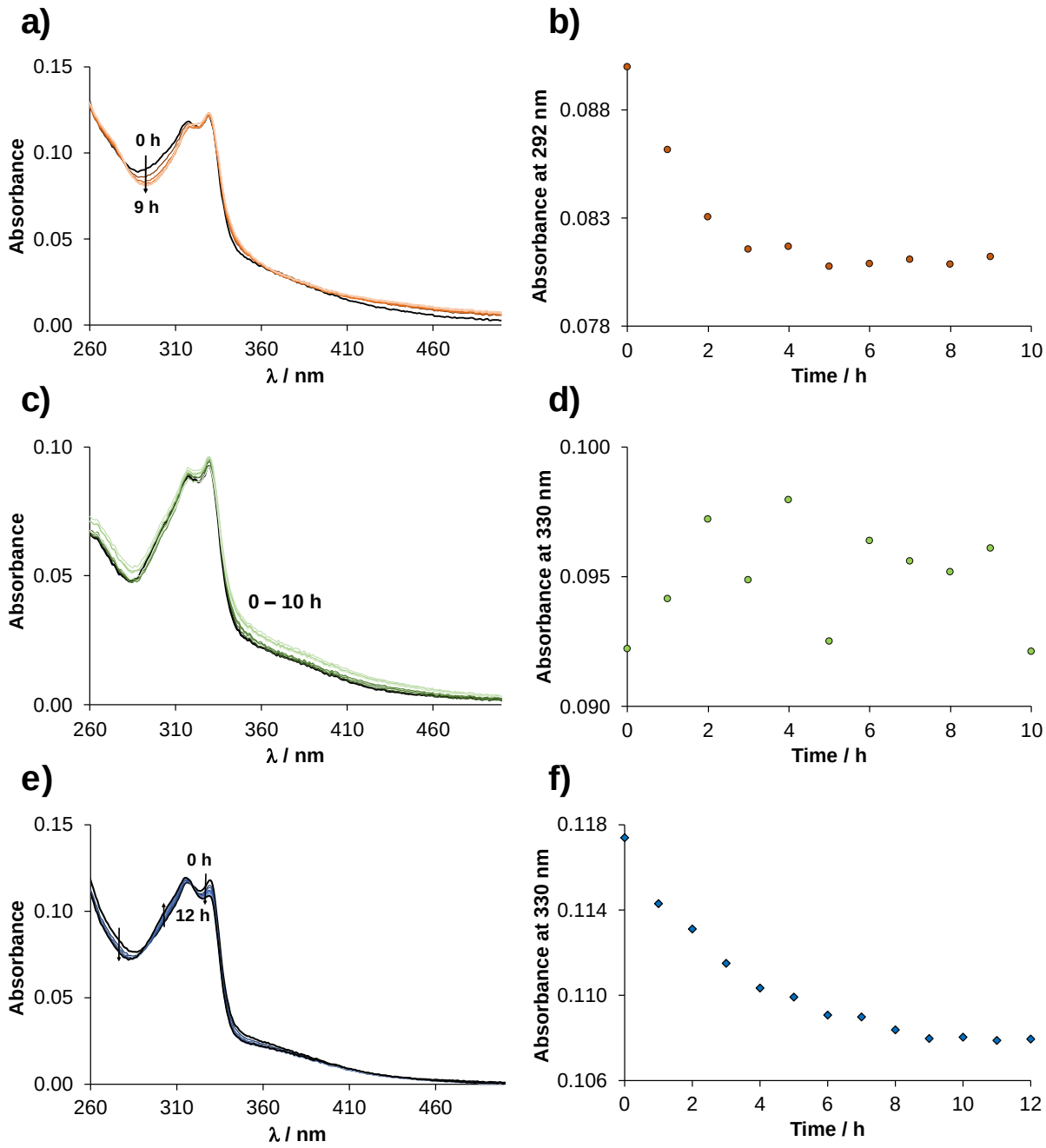

Figure S30. UV-vis spectra of [Re(CO)$_3$(4-Me-bpy-St-OH)Cl] (**5**) in 30% (*v/v*) DMSO/H_2O at a) pH = 5.1; c) pH = 7.0 and e) pH = 12.2 followed in time. Absorbance values at 292 (b) or 330 nm (d, f) for the same systems, respectively. {$c_{(5)}$ = 10 μM; *T* = 25.0 °C; ℓ = 1 cm; 30% (*v/v*) DMSO/H_2O; PBS' buffer (pH = 7.0)}.

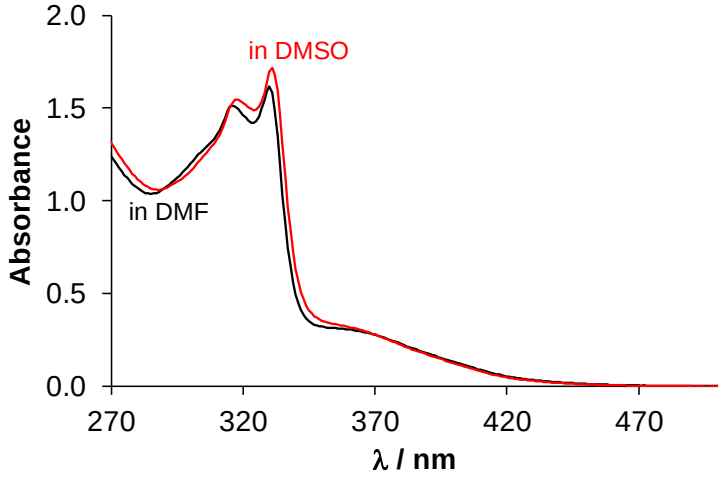

Figure S31. UV-vis spectra of $[Re(CO)_3(4\text{-Me-bpy-St-OH})Cl]$ (**5**) in DMF and DMSO. {$c_{(5)}$ = 100 μM; *T* = 25.0 °C; ℓ = 1 cm}

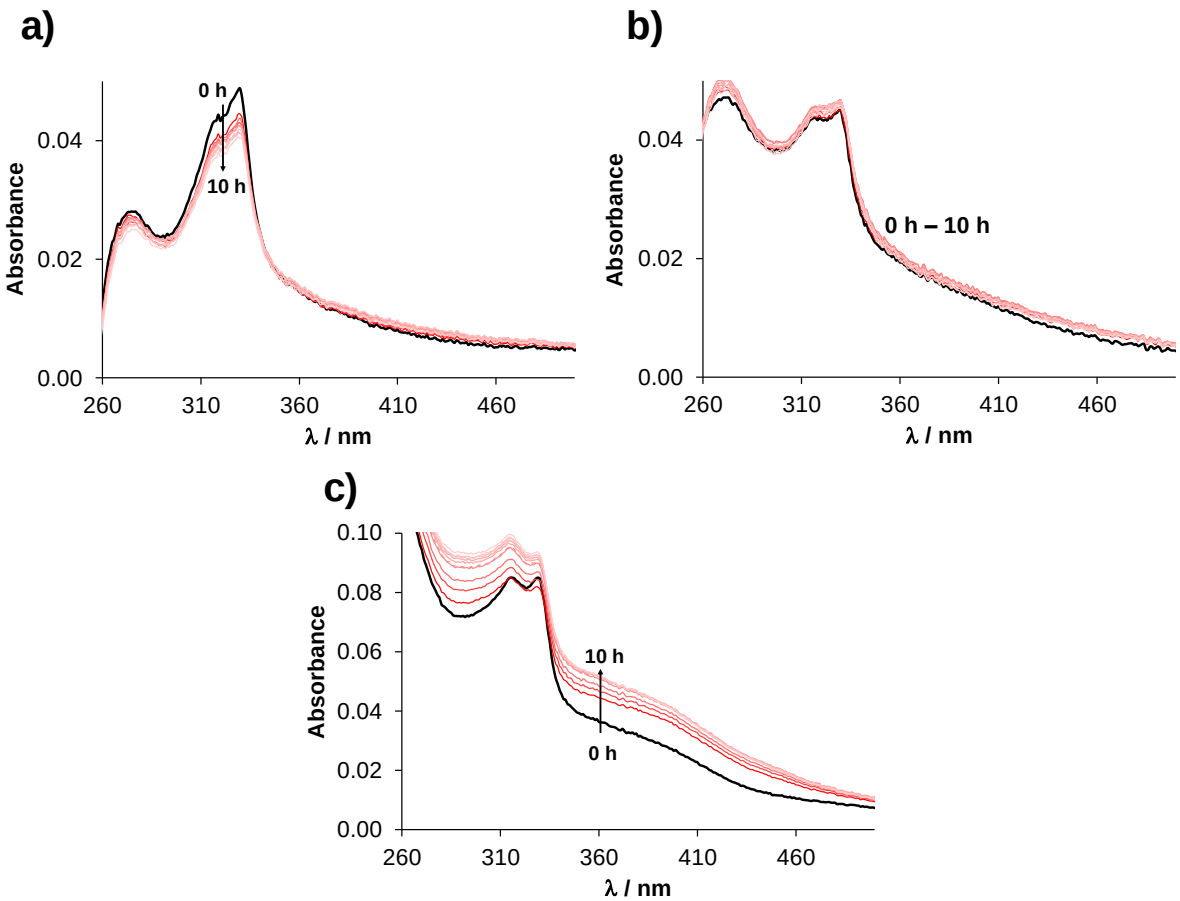

Figure S32. UV-vis spectra of $[Re(CO)_3(4\text{-Me-bpy-St-OH})Cl]$ (**5**) in 30% (*v/v*) DMF/H_2O mixture at a) pH = 1.9; b) pH = 4.9 and c) pH = 11.2 followed in time. {$c_{(5)}$ = 8 μM; *T* = 25.0 °C; ℓ = 1 cm; 30% (*v/v*) DMF/H_2O}.

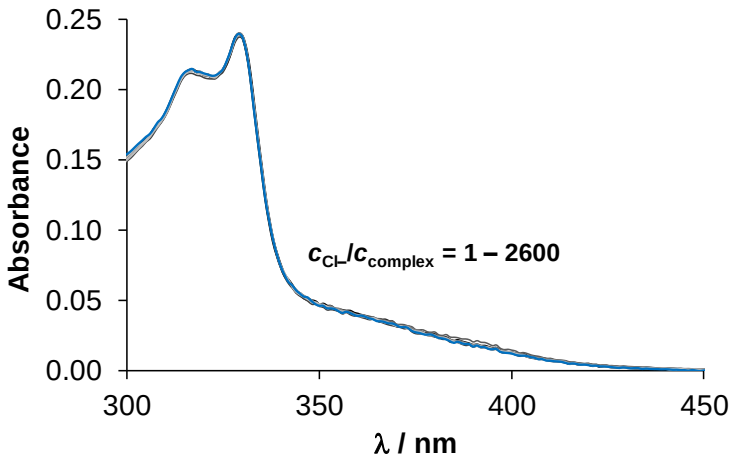

Figure S33. UV-vis spectra of [Re(CO)$_3$(4-Me-bpy-St-OH)Cl] (**5**) in 60% (*v/v*) DMF/H_2O mixture at increasing chloride ion concentration at pH 7.40. {$c_{(5)}$ = 14 μM; *T* = 25.0 °C; ℓ = 1 cm; 60% (*v/v*) DMF/H_2O}

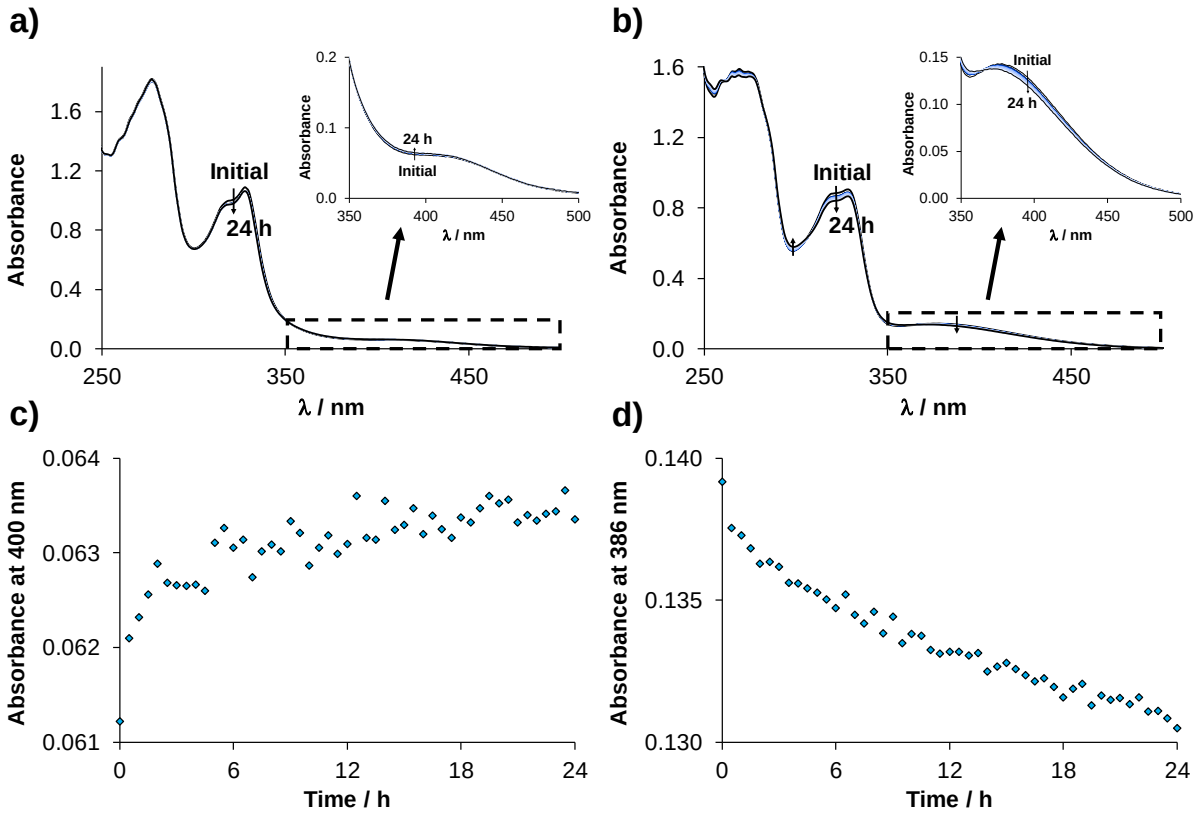

Figure S34. UV-vis spectra of (a) [RuCym(4-Me-bpy-St-OH)Cl]Cl (**3**) complex and (b) [RhCp*(4-Me-bpy-St-OH)Cl]Cl (**1**) in the presence of half equiv. HSA followed in time. Inset shows the charge-transfer region (350 – 500 nm) of the complexes. Absorbance values at (c) 400 nm and (d) 386 nm as a function of time for the same RuCym and RhCp* complex, respectively. {$c_{complex}$ = 70 μM; c_{HSA} = 35 μM; pH = 7.40 (PBS' buffer); ℓ = 1 cm; *T* = 25.0 °C}

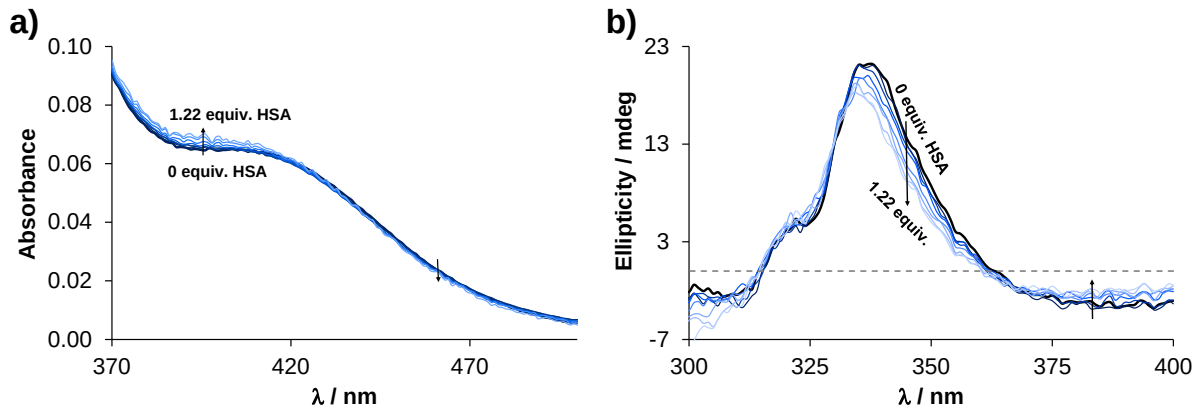

Figure S35. (a) UV-vis spectra and (b) CD spectra of [RuCym(4-Me-bpy-St-OH)Cl]Cl complex (**3**) in the absence and presence of various equivalents of HSA. {$c_{(3)}$ = 86 μM; c_{HSA} = 0 – 105 μM; pH = 7.40 (PBS' buffer); ℓ = 1 (UV–vis) or 0.5 (CD) cm; T = 25.0 °C}

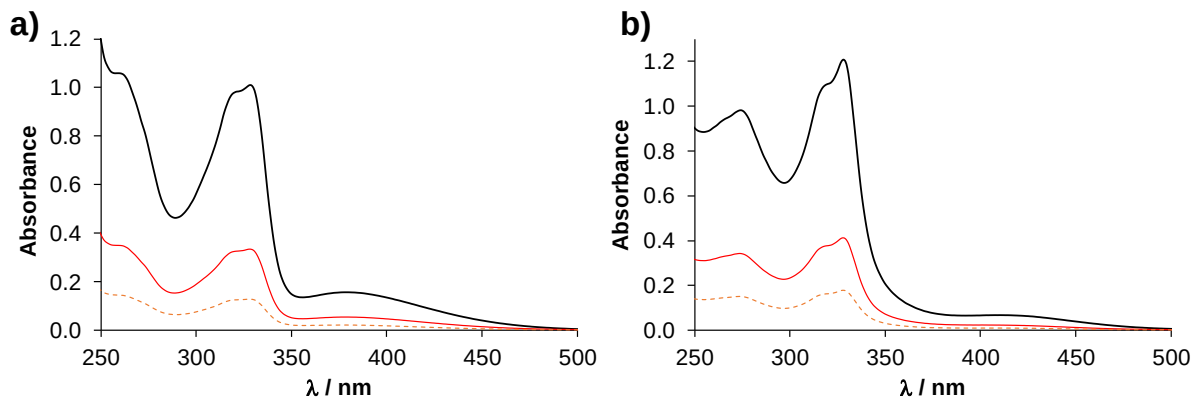

Figure S36. UV-vis spectra of ultrafiltrated (a) [RhCp*(4-Me-bpy-St-OH)Cl]Cl (**1**) and (b) [RuCym(4-Me-bpy-St-OH)Cl]Cl (**3**) complexes in the absence (red solid line) and presence of HSA (orange dashed line) along with the nonfiltered reference spectrum (black solid line). {$c_{complex}$ = 71 μM; c_{HSA} = 35 μM; pH = 7.40 (PBS' buffer); ℓ = 1 cm; T = 25.0 °C}

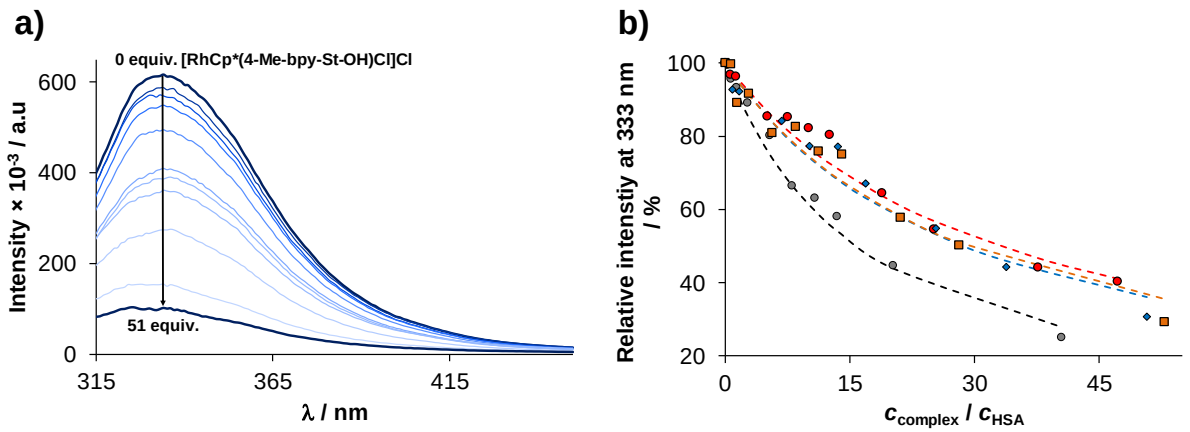

Figure S37. (a) Fluorescence emission spectra of HSA in the absence and presence of various amount of [RhCp*(4-Me-bpy-St-OH)Cl]Cl complex (**1**). (b) Experimental and calculated (dashed lines) relative emission intensities of HSA at 333 nm in the presence of various amounts of [RhCp*(4-Me-bpy-St-OH)Cl]Cl (**1**) (●), [RhCp*(4-Ph-bpy-St-OH)Cl]Cl (**2**) (●), [RuCym(4-Me-bpy-St-OH)Cl]Cl (**3**) (♦) and [RuCym(4-Ph-bpy-St-OH)Cl]Cl (**4**) (■) complexes. {c_{HSA} = 1 μM; $c_{complex}$ = 0 – 53 μM; λ_{EX} = 295 nm; pH = 7.40 (PBS' buffer); T = 25 °C; ℓ = 1 cm}

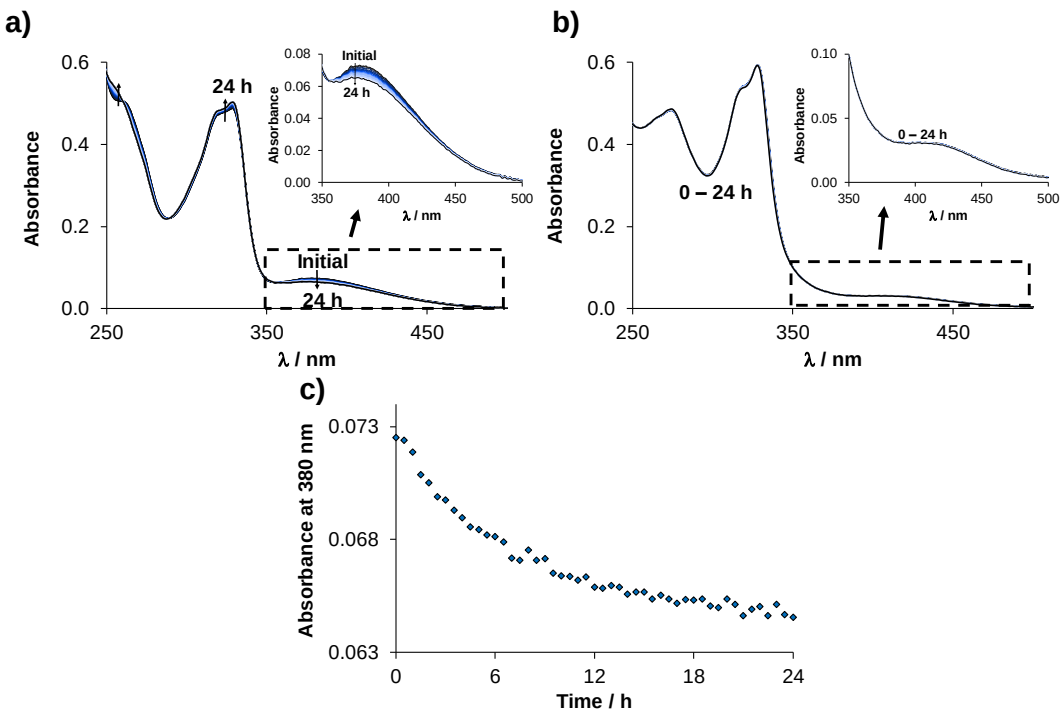

Figure S38. UV-vis spectra of (a) [RhCp*(4-Me-bpy-St-OH)Cl]Cl (**1**) and (b) [RuCym(4-Me-bpy-St-OH)Cl]Cl (**3**) in the presence of 10 equiv. MIM followed in time. Inserted figure shows the charge-transfer region (350 – 500 nm) of the complexes. (c) Absorbance values at 380 nm as a function of time for (**1**). {$c_{complex}$ = 35 μM; c_{MIM} = 350 μM; pH = 7.40 (PBS' buffer); ℓ = 1 cm; T = 25.0 °C}

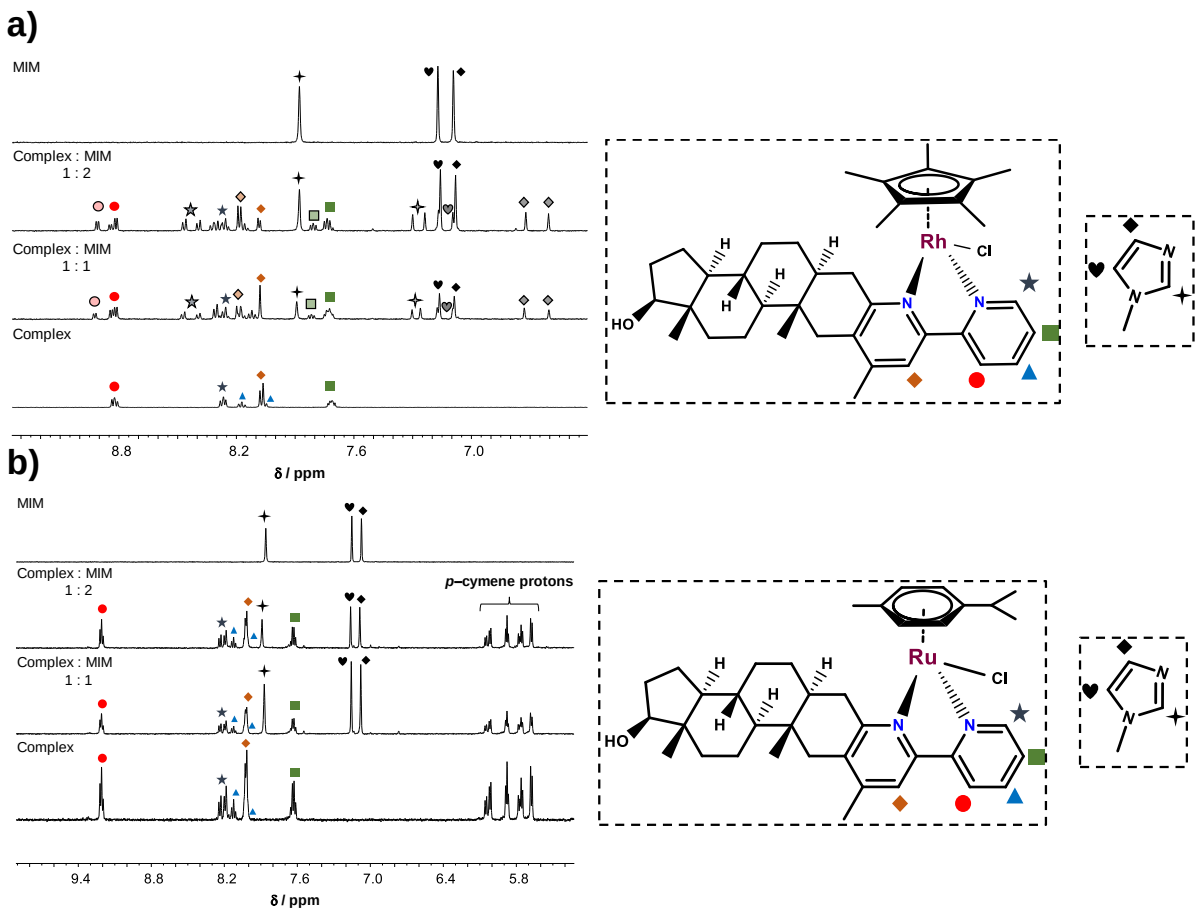

Figure S39. ^{1}H NMR spectra of (a) [RhCp*(4-Me-bpy-St-OH)Cl]Cl (**1**) and (b) [RuCym(4-Me-bpy-St-OH)Cl]Cl (**3**) complex alone or in the presence of 1 and 2 equiv. MIM in the low-field region. {$c_{complex}$ = 0.5 mM; c_{MIM} = 0.5 or 1.0 mM; pH = 7.40 (PBS' buffer); 10% (*v/v*) D_2O/H_2O; *T* = 25.0 °C}

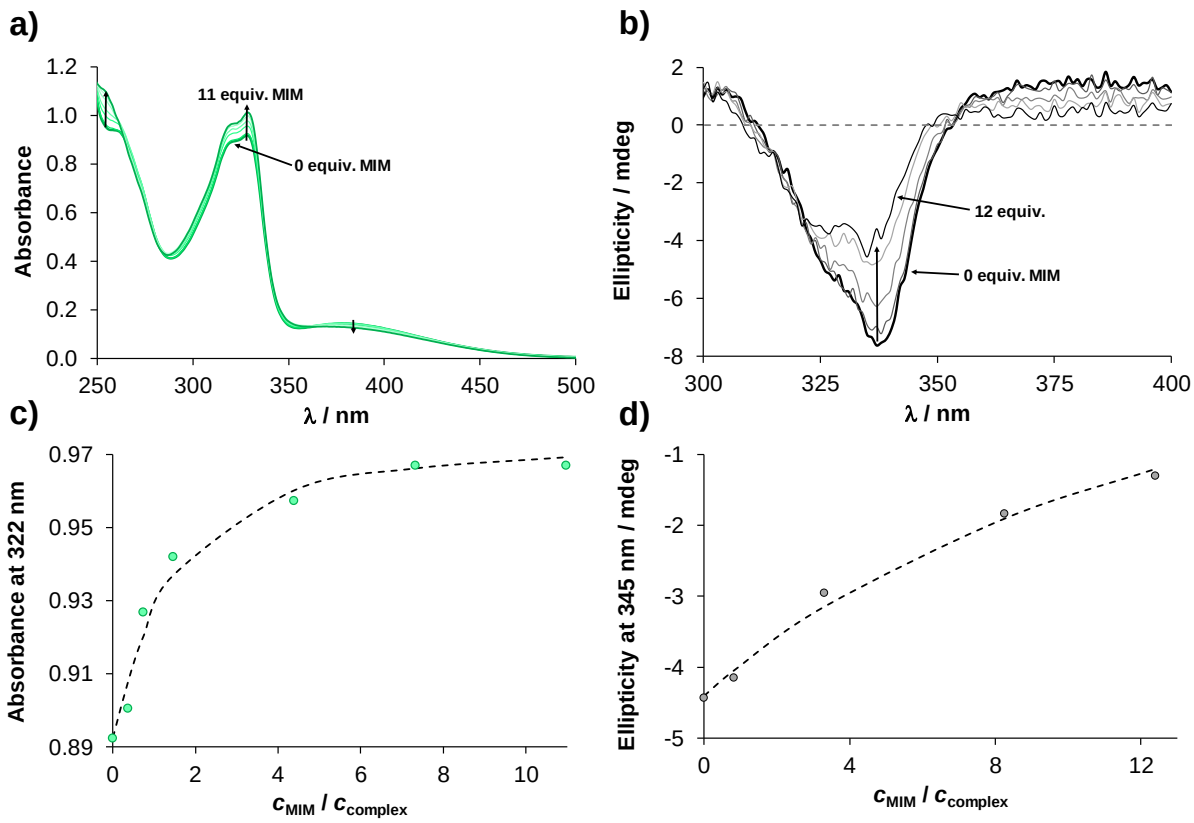

Figure S40. (a) UV-vis spectra of [RhCp*(4-Me-bpy-St-OH)Cl]Cl (**1**) and (b) CD spectra of [RhCp*(4-Ph-bpy-St-OH)Cl]Cl (**2**) complex in the presence of various equivalents of MIM. (c) Absorbance values at 322 nm and (d) ellipticity values at 345 nm as a function of c_{MIM} / $c_{complex}$ ratio along with the fitted (dashed) lines for the same (**1**) and (**2**) complexes, respectively. {$c_{complex}$ = 63 or 71 μM; c_{MIM} = 0 – 781 μM; pH = 7.40 (PBS' buffer); ℓ = 1 cm (UV–vis) or 0.5 cm (CD); T = 25.0 °C}

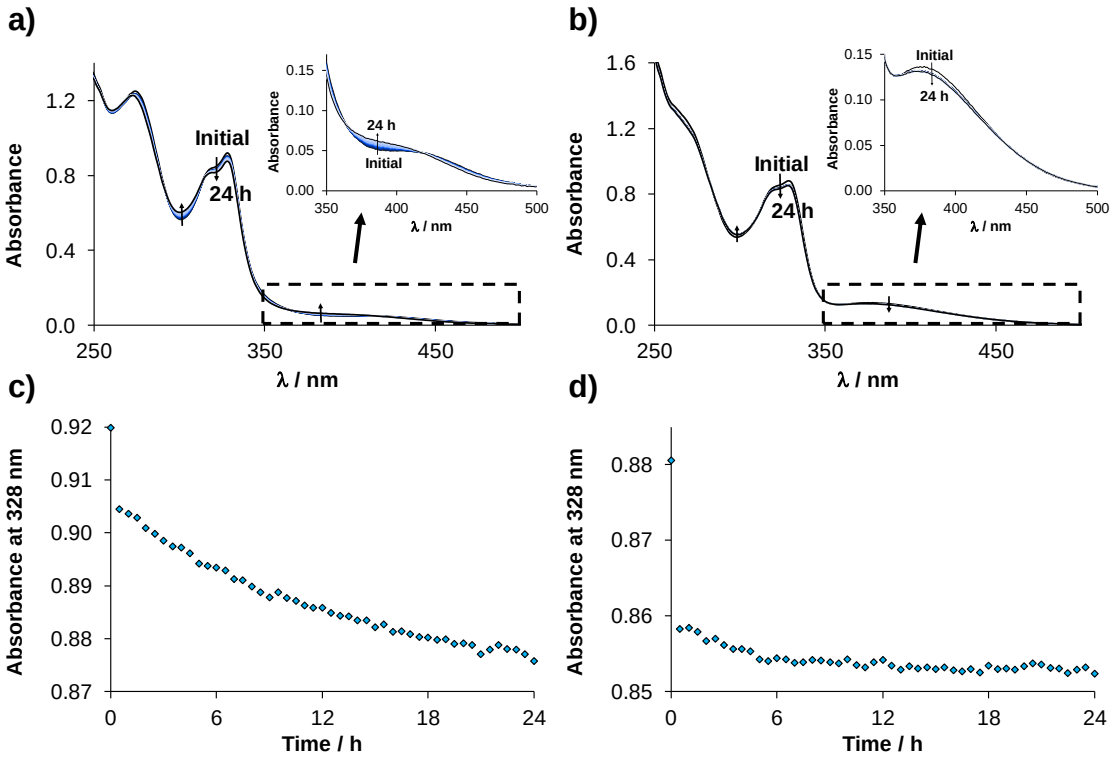

Figure S41. UV-vis spectra of (a) [RuCym(4-Me-bpy-St-OH)Cl]Cl (**3**) and (b) [RhCp*(4-Me-bpy-St-OH)Cl]Cl (**1**) complex in the presence of one equiv. guanine followed in time. Inset shows the charge-transfer region (350 – 500 nm) of the complexes. Absorbance values at 328 nm as a function of time for the same (c) (**3**) and (d) (**1**) complexes. {$c_{complex}$ = 70 μM; c_{HSA} = 70 μM; pH = 7.40 (20 mM phosphate buffer with 4 mM KCl); ℓ = 1 cm; T = 25.0 °C}

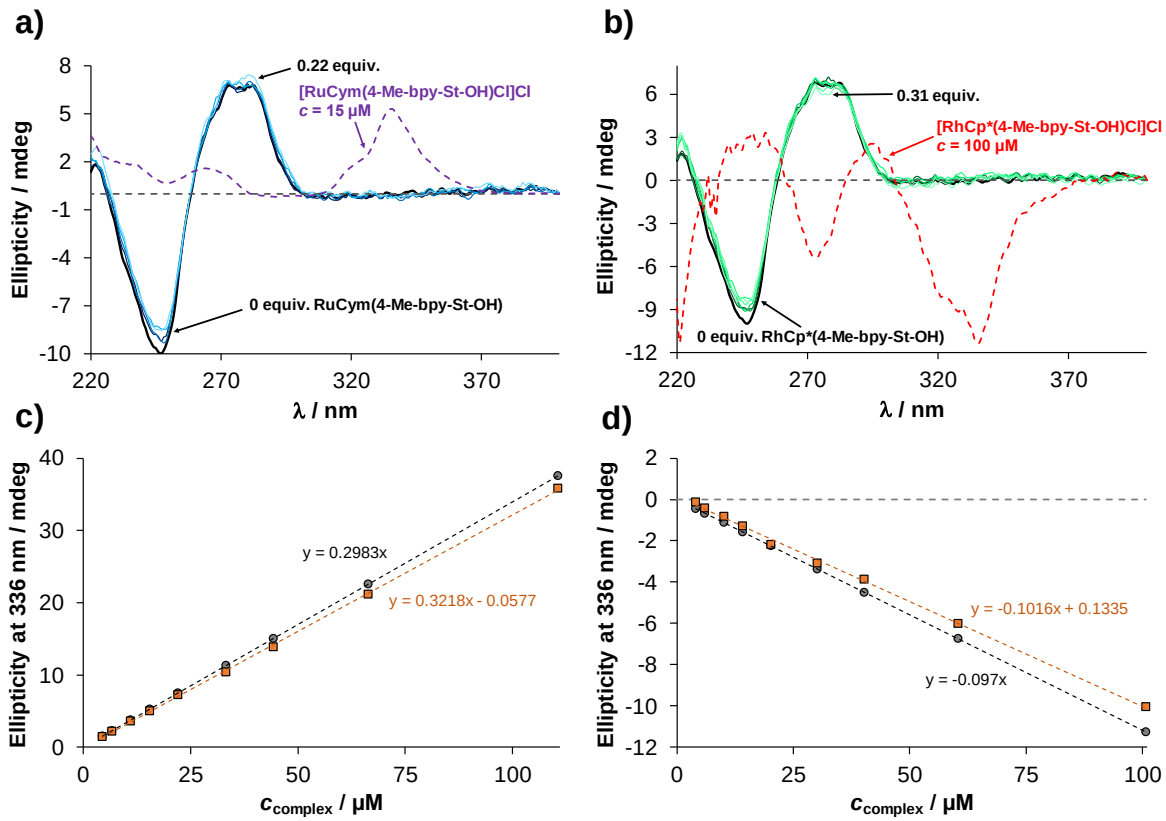

Figure S42. CD spectra of ct-DNA in the presence of various amounts of (a) [RuCym(4-Me-bpy-St-OH)Cl]Cl (**3**) and (b) [RhCp*(4-Me-bpy-St-OH)Cl]Cl (**1**) complex. The CD spectra of the individual complexes are also indicated (dashed lines). Ellipticity values at 336 nm as a function of $c_{complex}$ for the same (c) (**3**) and (d) (**1**) complexes in the absence (●) and presence (■) of ct-DNA. {c_{ct-DNA} = 98 μM; $c_{complex}$ = 0 – 100 μM; pH = 7.40 (20 mM phosphate buffer with 4 mM KCl); ℓ = 1 cm; *T* = 25.0 °C} *Note*: The CD spectra of ct-DNA were corrected with the spectra of the complexes at each point.

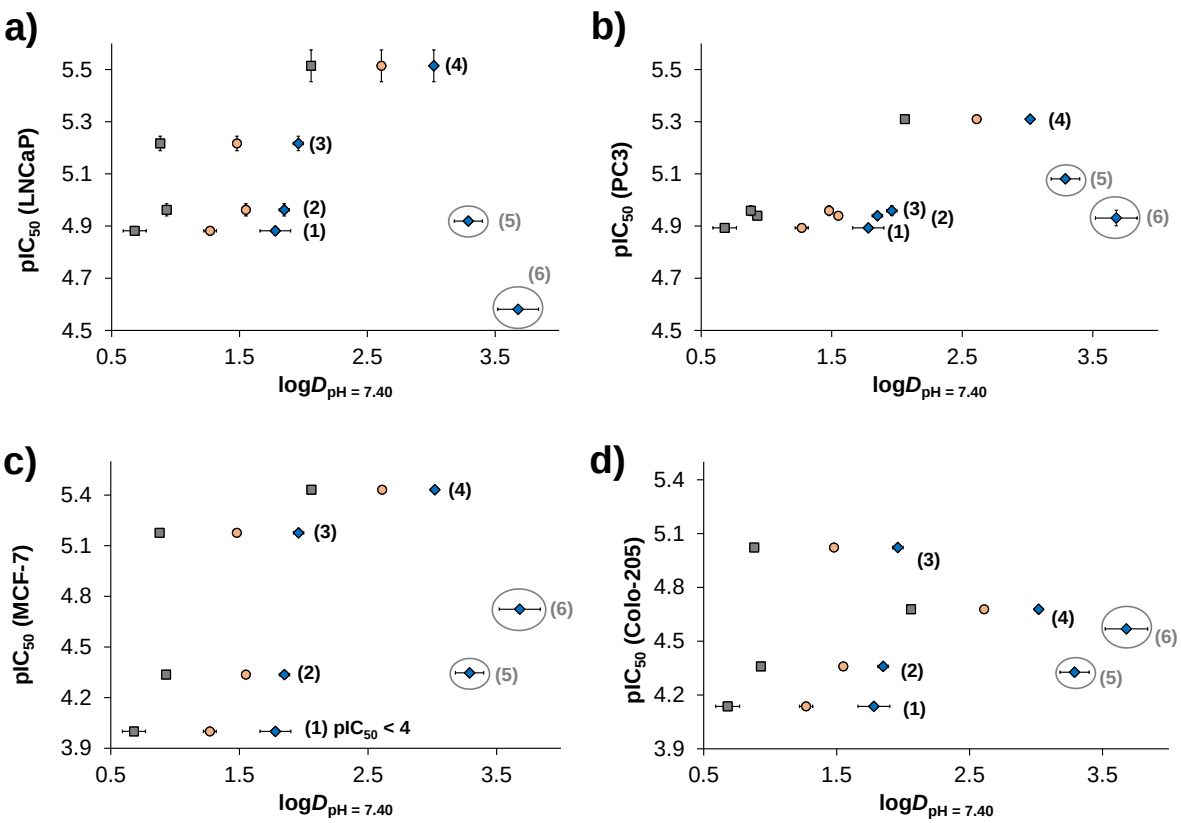

Figure S43. Correlation between the i*n vitro* cytotoxicity data (as $pIC_{50} = -\log IC_{50}$; where IC_{50} is expressed in mol/dm^3) and the distribution coefficients measured at pH 7.40 (as $\log D_{pH=7.40}$) of the organometallic complexes at the different chloride ion concentrations (4 mM: ■, 24 mM: ●, 100 mM: ♦) in (a) LNCaP, (b) PC3 (c) MCF-7 and (d) Colo-205 human cancer cell lines (incubation time: 72 h).